ABSTRACT

KIM, SOO KYUM. Mechanistic Study of Photodriven Intermolecular [2+2] Cycloaddition of Enones (Under the direction of Dr. Walter W. Weare and Dr. Felix N. Castellano.)

Since 2008, many photoredox catalysis have been developed in the organic synthetic community. However, mechanistic details of such reactions are often not fully elucidated and thus remain an area of debate. In particular, the specific chemical role of trialkylamines as reductive quenchers in photoredox catalysis is not fully appreciated. For example, trialkylammonium radical cations can initiate reduction chemistry as an alternative pathway to a typical photocatalytic cycle. Thus, a thorough investigation of trialkylamine radical cation reactivity is necessary to clarify the underlying mechanistic details for the observed photo-driven synthetic reactions.

To determine whether the reaction follows a standard photocatalytic cycle in absence of trialkylamines, a chemically inert reductive quencher, 4-*N,N*-dimethylaminotoluene (DMT) is used in the target photoreaction. Reaction does not proceed with DMT. Thus, the electron transfer steps for the proposed mechanism of the intermolecular [2+2] cycloaddition of enones were investigated with Stern-Volmer kinetics and a flash-quench method. Stern-Volmer kinetics verified the first electron transfer step, which corresponds to the proposed mechanism. Cyclic voltammetry and flash-quench experiments did not show a second electron transfer step of the proposed mechanism, confirming that the accepted pathway is incomplete.

To investigate the precise mechanism of the [2+2] cycloaddition, we investigated a trialkylamine radical cation and its downstream intermediate, α-amino radical. An α-amino radical was electrochemically characterized and identified as a reducing agent that is sufficiently reduce for reducing organic substrates. Attempts to reproduce the formation of cyclobutane using chemically generated α-amino radicals have not been successful. However, these attempts indicated the other downstream intermediate, an iminium ion, was not initiating the photodriven [2+2] cycloaddition. Overall, we conclude that photodriven intermolecular [2+2] cycloaddition of enones do not follow a standard photocatalytic cycle, and have ruled out one reaction pathway that involves an iminium ion.

Mechanistic Study of Photodriven Intermolecular [2+2] Cycloaddition of Enones

by
Soo Kyum Kim

A thesis submitted to the Graduate Faculty of
North Carolina State University
in partial fulfillment of the
requirements for the Degree of
Master of Science

Chemistry

Raleigh, North Carolina

2016

APPROVED BY:

David A. Shultz	Reza Ghiladi
Walter W. Weare Co-Chair of Advisory Committee	Felix N. Castellano Co-Chair of Advisory Committee

DEDICATION

This work is dedicated to my parents, Young Il Kim and Hark Soon Chang.

BIOGRAPHY

Soo Kyum Kim was born in Seoul, South Korea. He went to University of Illinois at Urbana-Champaign, where he obtained his Bachelor of Science in chemistry. During his undergraduate years, he joined Gewirth group and researched about photocatalysts that can be used in water splitting technology. Later, he attended North Carolina State University for advanced degree and graduated with Master of Science in Chemistry. During his graduate years, his researched about the mechanistic details of photoredox catalysis.

ACKNOWLEGEMENT

I would like to thank my parents for their help and support.

I would like to thank both my advisors, Professor Walter W. Weare and Professor Felix N. Castellano for their guidance and supports throughout my research. I would like to thank all members of Weare group and Castellano group for their help. I also want to thank my committee members, Dr. David A. Shultz and Dr. Reza Ghiladi for their suggestions and feedback.

I also would like to thank my friends, who shared meaningful and enjoying memories.

TABLE OF CONTENTS

LIST OF TABLES

LIST OF FIGURES

ABBREVIATIONS

bpy	2,2'-bipyridine
DIPEA	Diisopropylethylamine
DMF	Dimethylformamide
DMT	4-*N,N*-dimethylaminotoluene
dsbp	2,9-Di(sec-butyl-1,10-phenanthroline)
IR	Infrared
k_{et}	Electron transfer rate constant
k_q	Quenching rate constant
K_{sv}	Stern-Volmer constant
MeCN	Acetonitrile
MVK	Methyl vinyl ketone
MVKLA	Lithium coordinated methyl vinyl ketone
PPK	Phenyl 1-propenyl ketone
PPKLA	Lithium coordinated phenyl 1-propenyl ketone
ppy	2-Phenyl pyridine
TBAPF6	Tetrabutyl ammonium hexafluorophosphate
TEA	Triethylamine
UV	Ultra-Violet
vs $Fc^{+/0}$	Potential vs ferrocenium/ferrocene
vs SCE	Potential vs saturated calomel electrode

PART I: Literature Review

Introduction

Photochemical reactions are different in nature from thermal reactions. Photoexcited molecules exhibit distinctly different reactivity from their corresponding ground states. Photochemical reactions can provide access to both singlet and triplet states, while conventional thermally activated reactions are typically limited to singlet states.[1–5] Many synthetic limitations of thermal reactions, such as cycloaddition and Norrish type reaction, can be overcome by using these different reactivity and unique properties of excited molecule.[1–5] Despite the utility of photochemical reactions, photo-driven organic synthesis has developed slowly due to the inability of many organic molecules to absorb visible light.[6,7] Therefore, applications of photochemical organic reactions were traditionally limited to UV photolysis.[8]

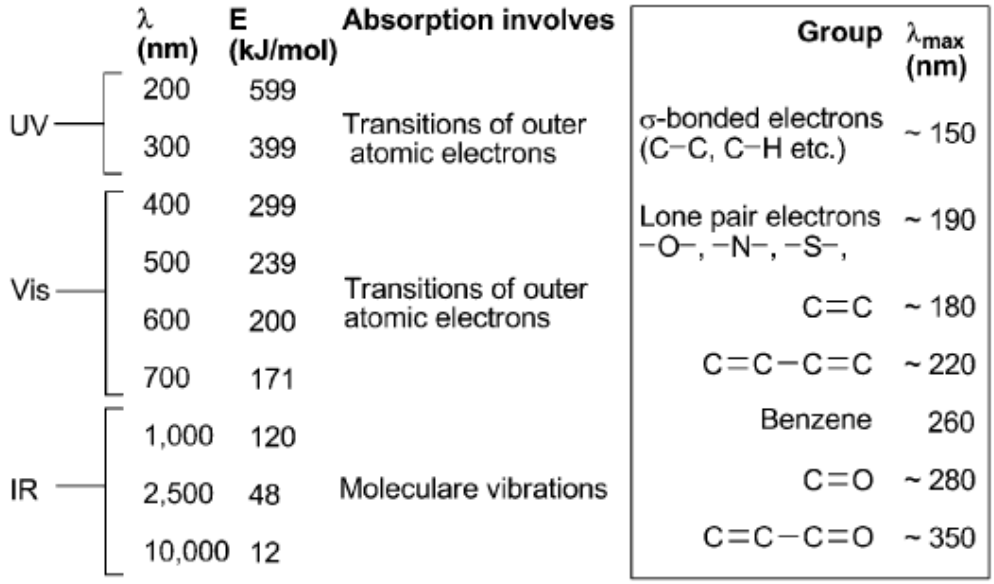

Figure 1. Absorption energies of various organic functional groups[6]

UV photolysis has significant drawbacks in photochemical organic reactions, which has limited its broad applications. UV light has high energy, which can break bonds as shown in Figure 1. The ability of breaking bonds makes the UV photolysis to be useful synthetic tool, however, because of its powerful nature, it often goes uncontrollable to lead side reactions or to decompose product.[6,7] To overcome this obstacle, several groups, who were

inspired by the natural photosynthesis, introduced photoredox catalysis as a method for organic synthesis.[9–11]

Photoredox Catalysis

Photoredox catalysis relies upon harnessing visible light and converting that photo-energy into chemical reactivity.[12] This is done by inserting an additional component, a photosensitizer that allows an alternative pathway to activate redox reactivity of organic substrates. Through this methodology, a photoredox catalytic cycle will avoid direct excitation of the organic substrate. This avoids the relatively harsh experimental conditions of UV photolysis to relative mild and controllable conditions where only visible light is used. With this advantage, photoredox catalysis can promote the design of novel chemical reactions, which couldn't be achieved using either thermal reaction or UV photolysis.[8,12]

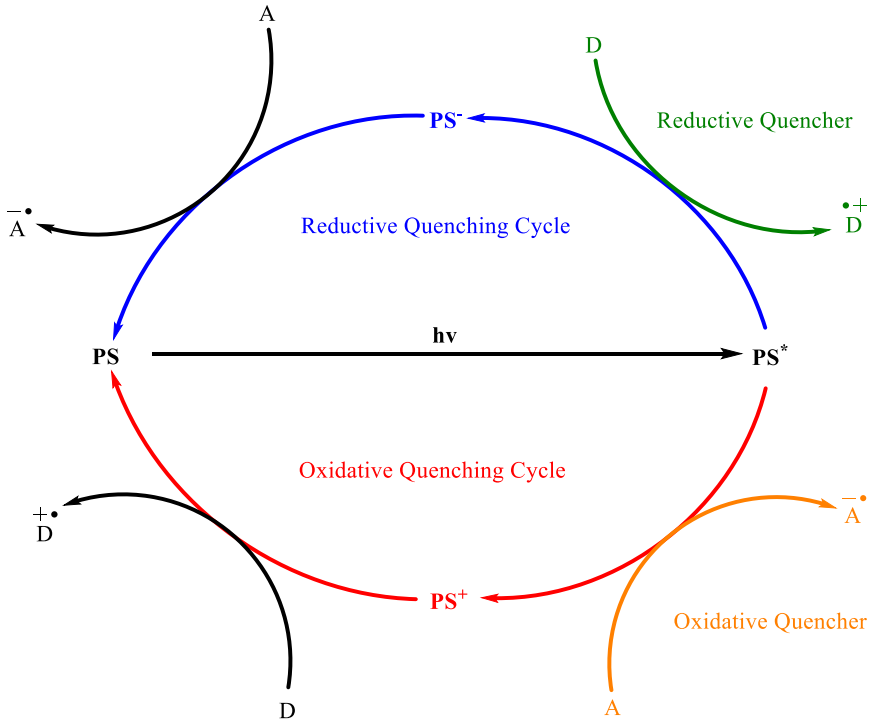

Figure 2. Photoredox diagram (PS: photosensitizer, A: electron acceptor, D: electron donor, hv: visible light excitation)

A photoredox system can be described as a catalytic cycle (Figure 2) with three main processes: 1) photo-excitation, 2) redox chemistry, and 3) regeneration of the ground state. In

photo-excitation, a photosensitizer is selectively excited with an appropriate wavelength. This excited photosensitizer initiates a redox process, where the excited photosensitizer is reduced (reductive quenching cycle) or oxidized (oxidative quenching cycle) by quencher. Finally, the ground state photosensitizer is regenerated via a single electron transfer from reduced or oxidized photosensitizer to organic substrates.

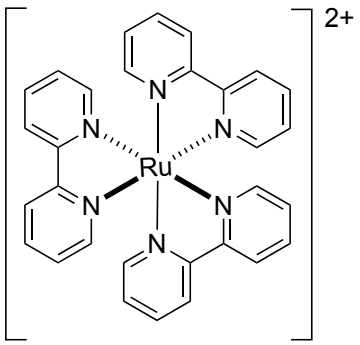

Figure 3. The bench mark photosensitizer: $[Ru(bpy)_3]^{2+}$

In photoredox catalysis, a photosensitizer is responsible for harnessing visible light and activating redox processes. A suitable photosensitizer in photoredox catalysis need excited state with following characteristics: 1) ability to absorb visible light, 2) a high quantum yield, 3) sufficiently long lifetime to undergo chemical reactions, and 4) redox potentials that react with targeted substrates. Due to these requirements, early photoredox catalysis extensively used tris-2,2-bipyridyl Ruthenium^{II}, for its well-studied photophysical properties. As shown in Figure 3, $[Ru(bpy)_3]^{2+}$, one of the most researched photosensitizers, is a benchmark photosensitizer. With a relative strong metal to ligand charge transfer (MLCT) absorption band, centered at 452 nm (ε = 14600 $cm^{-1}M^{-1}$), a long excited lifetime (1100 ns in acetonitrile) with high quantum yield (Φ = ~1), and favorable redox potentials, $[Ru(bpy)_3]^{2+}$ is an ideal photosensitizer for photoredox catalysis.[13–15]

In designing photoredox catalytic systems, the redox potential of each component is crucial. As shown in Figure 4, the reduction potential of the ground state ($E^{II/I}$ = – 1.68 V vs $Fc^{+/0}$) $[Ru(bpy)_3]^{2+}$ is significantly more negative than that of the excited state ($E^{II*/III}$ = – 1.20 V vs $Fc^{+/0}$).[16] Consequently, introducing stoichiometric amounts of reductive quenchers into $[Ru(bpy)_3]^{2+}$ mediated photoredox catalysis generates a strong reducing agent (Ru^{I} species), enabling the reductive reactivity. For oxidative photoredox catalysis, a similar concept is utilized, since the oxidation potential of the ground state ($E^{III/II}$ = 0.90 V vs $Fc^{+/0}$)

is more positive than that of the excited state ($E^{I/II*}$ = – 1.20 V vs $Fc^{+/0}$).[16] Thus, oxidation catalysis with $[Ru(bpy)_3]^{2+*}$ and appropriate oxidative quenchers generates $[Ru(bpy)_3]^{3+}$, which is a strong oxidizing agent and can drive oxidative reactivity.

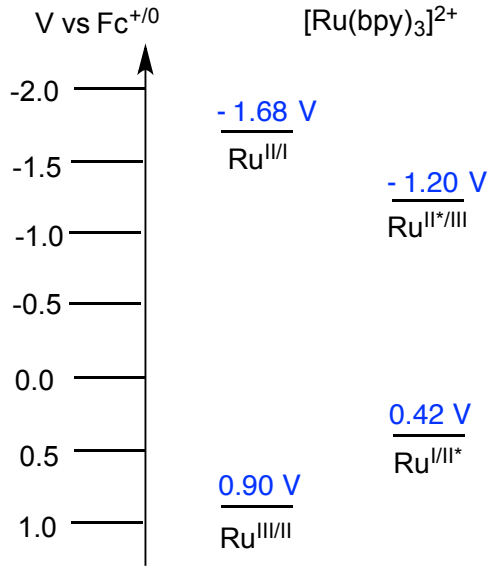

Figure 4. Redox potential of $[Ru(bpy)_3]^{2+}$

Quenchers should be carefully matched the redox properties of a given photosensitizer. The redox potential between excited photosensitizer and that of the quencher need to promote the single electron transfer from a quencher to a photosensitizer. Furthermore, the quenching rate constant (k_q) between the excited photosensitizer and the quencher needs to be much higher than k_q between the excited photosensitizer and other substrates. Lastly, the quenchers and their downstream products should be chemically inert if the role of the quencher is limited to sacrificial electron donor or acceptor. So far, various types of quenchers have been investigated and applied in photoredox catalysis. In oxidative quenching system, methyl viologen, persulfate ion, dinitrobenzenes, and aryldiazonium salts are useful oxidative quenchers.[17] In reductive quenching systems, tertiary amines are widely employed.[17]

Scope of Photoredox Catalysis and Mechanistic Debates

Photoredox catalysis for organic synthesis has promoted an intense growth in the field. In 2007, MacMillan, Yoon, and Stephenson groups reported photochemical reactions using

photoredox catalysis.[10,11,17–21] Using a reductively quenched photocatalytic cycle to generate enantioselective products inspired the synthetic community, and triggered a dramatic growth of the field as shown in Figure 5. However, despite this expansion of the field, only a few reported mechanistic investigations focused on electron transfer steps from reduced photosensitizer to organic substrates.[22–26] The lack of such mechanistic evidences opened the debates whether redox process of photosensitizer or chain propagation of the radical intermediate catalyzes the photoredox catalysis.

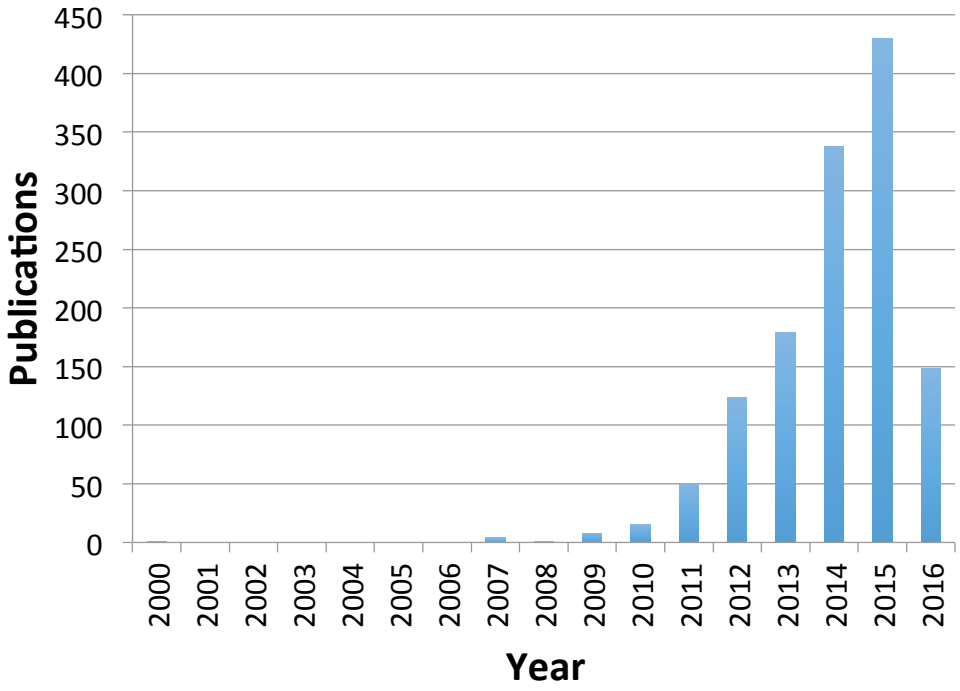

Figure 5. Number of publications in the span of 2000 – 2016 (From ISI web of Knowledge; as of 4/14/2016; keyword: 'Photoredox Catalysis')

One of the mechanistic concerns that will be discussed in this report is the use of tertiary amines in reductive photoredox catalysis. In reductive photoredox catalysis, reactions are only reproduced when trialkylamines are employed as reductive quenchers.[23,27] Other types of reductive quenchers show little or no reactivity. Due to this observation, the role of the trialkylamine is considered carefully along with the reactivity of trialkylamine radical cations, which are produced after donating an electron to the excited photosensitizer.

Reactivity of Trialkylamine Radical Cation

Trialkylamine radical cations are reactive species that can potentially form reactive downstream intermediates. As depicted in Figure 6, trialkylamine radical cations have various reactivity modes that are able to form intermediates such as α-amino radicals, iminium ion, and other free radicals.[28] These reactive downstream intermediates have potent to couple with electrophilic or nucleophilic compound and sometimes can act as a secondary reductant.[28] Thus the reactivity of downstream intermediates can lead to incorrect mechanistic interpretation. Consequently, the formation of radical cations raises questions about the true origin of reductant in reductively quenched photoredox catalysis. In the following section, three primary reactivity modes, including deprotonation, hydrogen atom abstraction, and C-C cleavage, of trialkylamine radical cation will be discussed.[25,28]

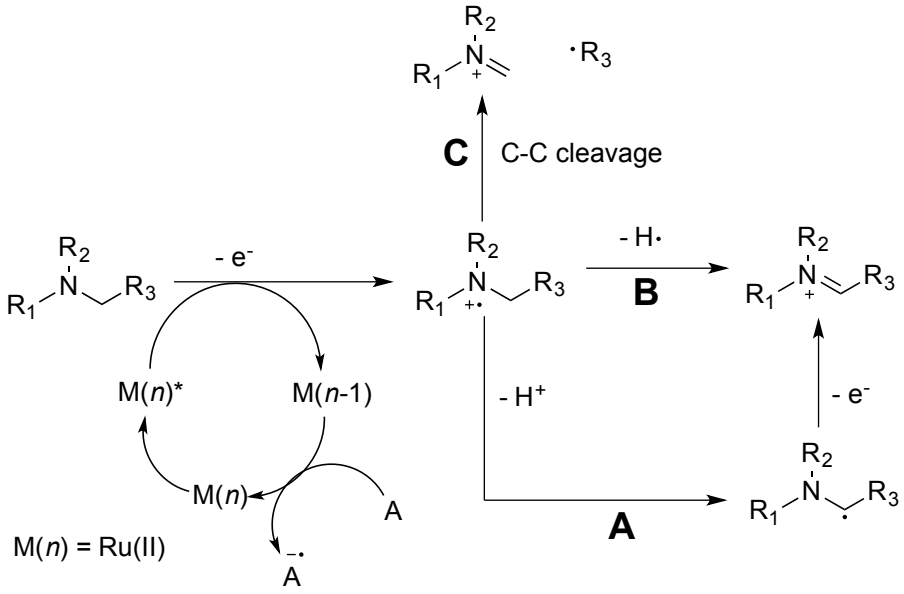

Figure 6. Possible reactivity modes of trialkylamine radical cations (A: formation of α-amino radicals, B: formation of iminium ions, C: C-C cleavage)

Trialkylamine radical cations can transform to α-amino radicals, which are generated through deprotonation from the amine radical cation.[29–32] When a trialkylamine is oxidized, a substantial increase in acidity occurs, accompanied by a significant weakening of the α-C-H bond. In case of triethylamine, the pK_a is about ~40 in acetonitrile, but decreases to 14.7 in the trialkylamine radical cation.[25,33] Therefore, the formation of amine radical cations weaken

the bond dissociation energy of the C-H bond from 90.7 kcal/mol to 42 kcal/mol.[25,34] This weakened α-C-H bond, coupled with the increased acidity of triethylamine radical cation, allows the formation of α-amino radicals upon deprotonation at α-position.[30,33] The resulting α–amino radical is known to be highly reactive species, being both a nucleophilic compound and a strong reducing agent (E_{ox} = – 1.12 V vs SCE).[34] The nucleophilicity of the α–amino radical can result in reaction with electrophiles such as Michael acceptors.[25,28,29] Using this reactivity, several groups have reported photo-driven α–amino radical coupling reactions.[35–39]

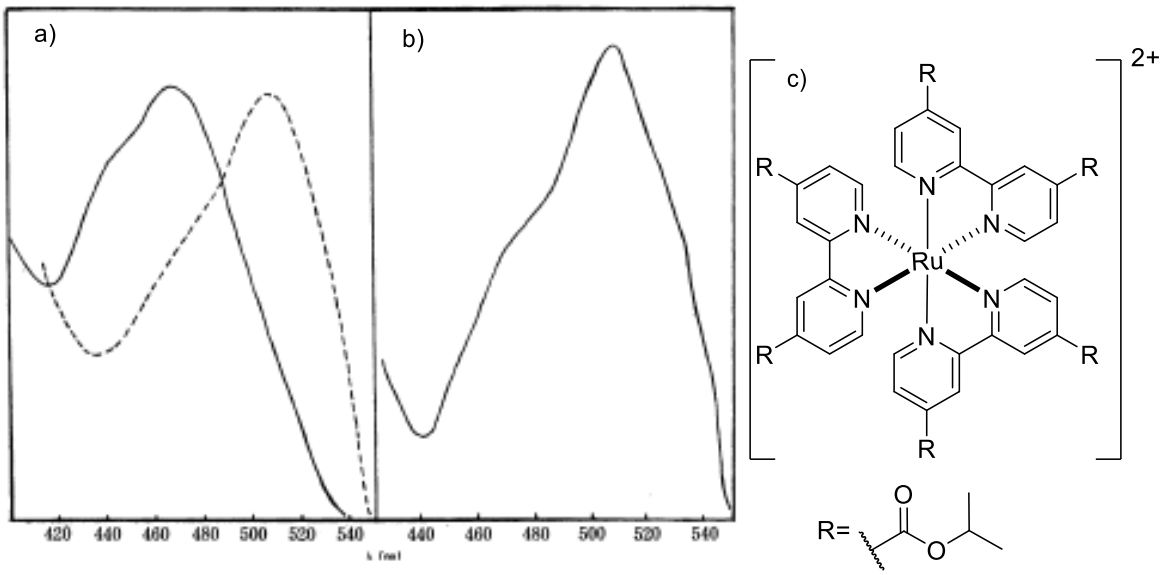

Figure 7. a) solid line – electronic absorption spectrum of hydrophobic Ru(II) complex before irradiation, dashed line – spectrum of hydrophobic Ru(II) complex after irradiation; b) one electron reduction product of Ru(II) complex; c) hydrophobic Ru(II) complex[40]

The strong reducing ability of the α-amino radical can be an electron donor and reduce substrates in a variety of reactions. For instance, an α–amino radical can reduce a ground state photosensitizer, reacting net two electrons from one photon. As shown in Figure 7, Whitten *et al.* reported such a secondary reduction by α–amino radical showing that the absorption spectra of a ground state Ru(II) polypyridyl complex shifts upon absorption.[41] This is mechanistically shown in Figure 8, where α-amino radical is oxidized to the form an iminium ion.[41]

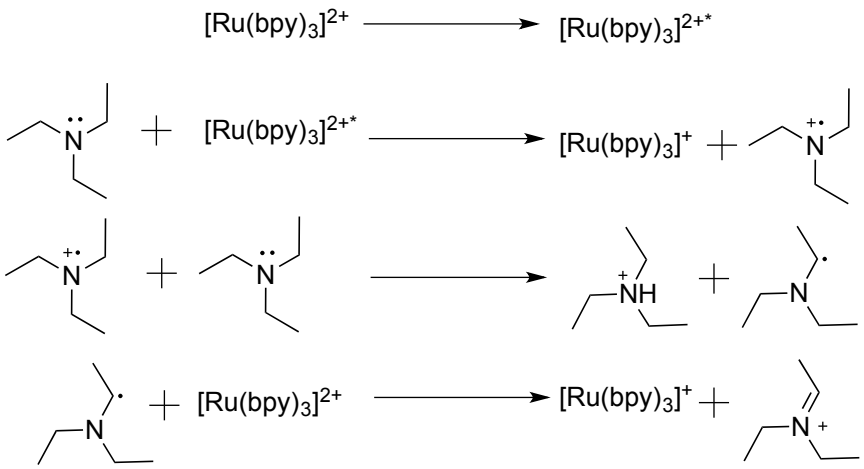

Figure 8. Mechanism of secondary reduction of photosensitizer by amine radical cation

The trialkylamine radical cation could form iminium ions, which are powerful electrophiles.[33,42–44] An iminium ion can be generated in two different pathways, either by directly hydrogen atom abstraction or indirectly oxidation of an α–amino radical.[28,33] Hydrogen atom abstraction is observed when a good hydrogen atom acceptor is present in the reaction system. Alternatively, an iminium ion forms after oxidation of an α–amino radical, as shown in Figure 8.[40,45] Both pathways forms a powerful electrophilic substances, and its reactivity have been applied to derive many reactions, such as Mannich reaction, Aza-Henry reaction, etc.[43,46]

Lastly, trialkylamine radical cation can undergo β-scission of a C–C bond, producing an iminium ion and a free radical. Trialkylamines with longer alkyl group undergo this process cleaving the C-C bond α to the nitrogen atom to produce neutral carbon radicals and an iminium ion.[47] The presence of the reactive free radical and electrophile in system potentially initiates the uncontrolled reaction. However, such β-scission of C–C bond requires some conditions, such as presence of ether in solution, C–C bond cleavage is rare for simple trialkylamines (such as DIPEA and TEA).[48]

Diverse reactivity of trialkylamine radical cations requires closer investigation of its proposed mechanism. As shown in Figure 8, the downstream reaction of amine radical cation results in the formation of both nucleophilic and electrophilic intermediates. The presence of a secondary reducing agent must be considered when reaction mechanisms are proposed, since the reducing agent is projected to have a relatively strong reduction potential compared to that of the reduced photosensitizer, such as $[Ru(bpy)_3]^+$ and *fac*-$[Ir(ppy)_3]^-$.

Intermolecular [2+2] Cycloaddition of Enones

With the complex reactivity of trialkylamine radical cations in need, we selected one of reductively quenched photoredox system for investigation of the mechanistic process of photoredox catalysis. The photo-driven [2+2] cycloaddition of intermolecular enones, which was reported by Yoon and co-workers in 2009, was chosen.[9] The photo-driven [2+2] cycloaddition of enones are inspired by the work of Krishe and co-workers, who reported a [2+2] cycloaddition of bisenone via single electron reduction using copper and cobalt catalysts.[49,50] Du *et al* developed photo-driven [2+2] cycloaddition of bisenone in 2007 expanding the scope of the reaction to include intermolecular enones in 2009.[9,18]

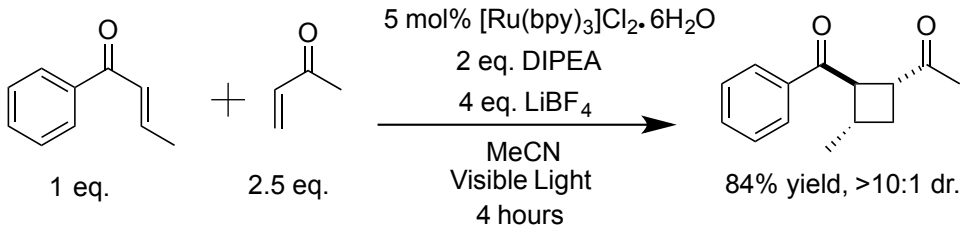

Figure 9. Intermolecular [2+2] cycloaddition of enones by Yoon[9]

General Mechanism of [2+2] Cycloaddition

In a typical [2+2] photocycloaddition between enone and alkene, an enone triplet excited state is generated to initiate cycloaddition. As shown in Figure 10, upon absorption by the enone, an electron gets promoted into the π^* orbital of enone.[51] Typically, α, β – unsaturated enones were used to achieve a long-lived excited state.[51–53] With a long-lived excited state, the enone singlet excited state undergoes intersystem crossing (ISC) to form a triplet excited state. The energy gap between the π orbitals in the triplet excited state of enone and electron-accepting substrate should be small to interact each other. Under these conditions, an exciplex between the triplet excited state of enone and electron-accepting substrate can be produced to form a triplet diradical compound. Subsequent intersystem crossing of the triplet diradical forms a singlet diradical, eventually leading to the formation of the targeted cyclobutane product.[51–54]

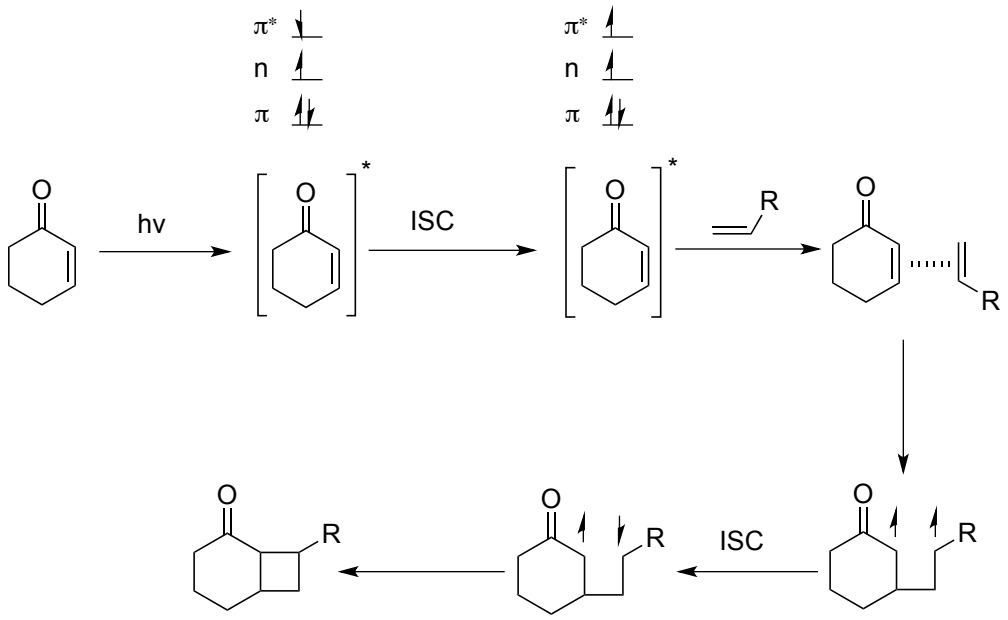

Figure 10. Mechanism of [2+2] cycloaddition of enone and alkene.[51]

However, [2+2] photocycloaddition of intermolecular enones has a limitation in the direct excitation, results in rapid deactivation by E/Z isomerization of the alkene.[12] The saturation of α position of enone shortened the lifetime of excited state that prohibited the coupling reaction. Inability of the desired coupling reactions as shown in Figure 11, UV photolysis of intermolecular enone does not produce any cyclobutane, but the mixtures results in E/Z isomerized products of phenyl 1-propenyl ketone and unreacted methyl vinyl ketone. This indicates that the electronically excited triplet aryl enone preferentially undergoes alkene isomerization, instead of coupling with Michael acceptor.[8]

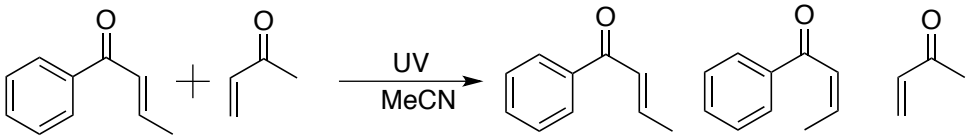

Figure 11. UV photolysis of phenyl 1-propenyl ketone and methyl vinyl ketone in acetonitrile

This synthetic limitation was overcome, when photoredox catalysis, which uses $[Ru(bpy)_3]^{2+}$, DIPEA as sacrificial electron donor, and $LiBF_4$ was applied to yield a trans - cyclobutane product with high yield (84 %) and excellent diastreoselectivity (d.r.>10: 1) as shown in Figure 9. Mild Lewis acids ($LiBF_4$) played important role, bonding to the carbonyl

and driving the lowering the reduction potential of bisenone.[9,18] Furthermore, this increases the stability of the radical anion intermediate. The additional synthetic challenge in intermolecular [2+2] cycloaddition was the prevention of homodimerization of aryl enones. This was overcome by using a less-conjugated Michael acceptor such as methyl vinyl ketone, which was an electrophilic substrate.[9]

Proposed Mechanism of [2+2] Cycloaddition of Intermolecular Enones

As shown in Figure 12, Yoon's proposed mechanism followed the general steps of a photoredox cycle.[55] Excited $[Ru(bpy)_3]^{2+*}$ is reductively quenched by DIPEA to form $[Ru(bpy)_3]^{+}$, which reduces lithium coordinated aryl enone. The reduction product undergoes a transformation to form an aryl ketyl radical anion. The aryl ketyl radical anion then couples with methyl vinyl ketone and undergoes a [2+2] cycloaddition to yield the cyclobutane radical. The final product is formed through the oxidation and detachment of Lewis acidic lithium.

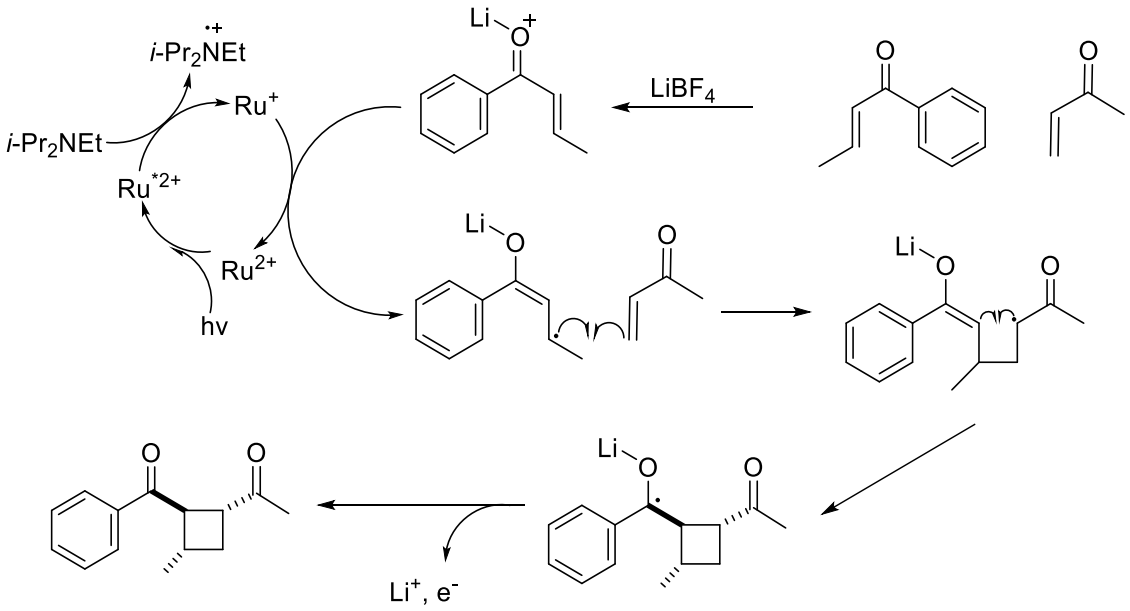

Figure 12. Mechanism of photodriven intermolecular [2+2] cycloaddition of enone.[9,55]

The proposed mechanism demonstrates the features of a general reductive quenching cycle, but we believed that the mechanism remains questionable due to the undefined role and reactivity of the trialkylamine radical cation. To investigate electron transfer process of

photoredox catalysis, a chemically inert reductive quencher, 4-*N,N*-dimethylaminotoluene (DMT) was chosen to replace trialkylamine in the photoredox cycle.[56,57] Using a chemically inert reductive quencher will indicate whether [2+2] cycloaddition of intermolecular enone is directly initiated by $[Ru(bpy)_3]^+$ or by a trialkylamine radical cation.

Chemically Inert Reductive Quencher: 4-*N,N*-dimethylaminotoluene (DMT)

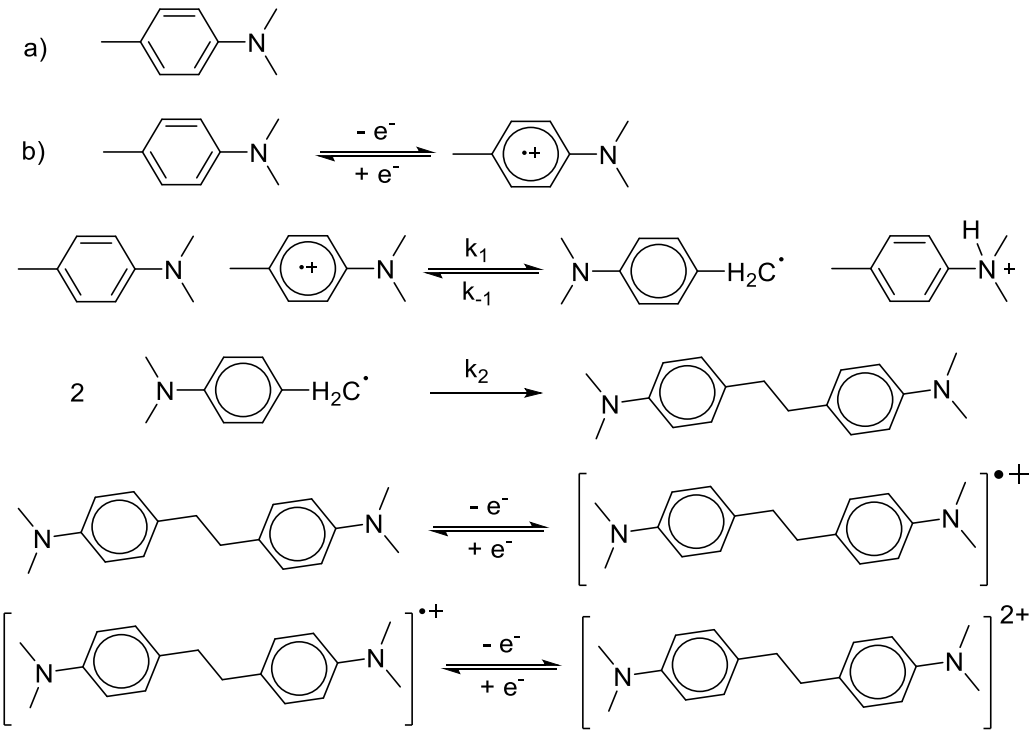

Figure 13. a) The structure of 4-*N,N*-dimethylaminotoluene (DMT); b) Mechanism of DMT dimerization.[57]

In order to avoid the side reactions triggered by highly reactive trialkylamine radical cations, the reductive quencher (DMT) can be used as an alternative sacrificial electron donor. DMT (0.31 V vs $Fc^{+/0}$) is a known reductive quencher that has suitable redox potential with excited $[Ru(bpy)_3]^{2+*}$ and allows electron transfer with a fast quenching rate constant (1.6×10^9 $M^{-1}s^{-1}$).[16,58] Unlike trialkylamine donors, when DMT was oxidized, the amine radical cation, DMT•+ reacts with another DMT to form a dimerized product (Figure 13). This dimerization process makes DMT unable to initiate additional radical reactions at first reported and examined by Oyama and co-workers.[57] The mechanism of DMT dimerization

follows an $EC_{rev}C_2EE$ two electron oxidation mechanism.[57] DMT dimer can also serve as a sacrificial electron donor, since it has an almost identical redox potential to that of the DMT. Oxidized DMT dimer is believed to be chemically inert.

Exploiting these properties, DMT can be used as a sacrificial electron donor in photoredox cycles.[16,35] Thus, we propose that DMT will allow us to investigate the individual electron transfer steps of [2+2] cycloaddition of intermolecular enones in the absence of any radical side reactions, such as those present with trialkylamine electron donors.

PART II. Results and Discussion

1. Control Experiments

A chemically inert reductive quencher, DMT, is used to examine whether the photochemical products can be formed in absence of trialkylamine radical cation. We predict that if the reaction mechanism follows a standard photocatalytic cycle, then the results will be reproducible with alternative quenchers such as DMT. An inability to form product would indicate that there is an alternative reaction pathway that initiate the [2+2] cycloaddition reaction. Alternative photosensitizers and alternative sacrificial electron donors are therefore used to investigate the role of trialkylamine for this photoredox reaction. During these control experiments, the molar ratio of PPK (**1**), MVK (**2**), and $LiBF_4$, were kept consistent with the known optimized conditions.[9]

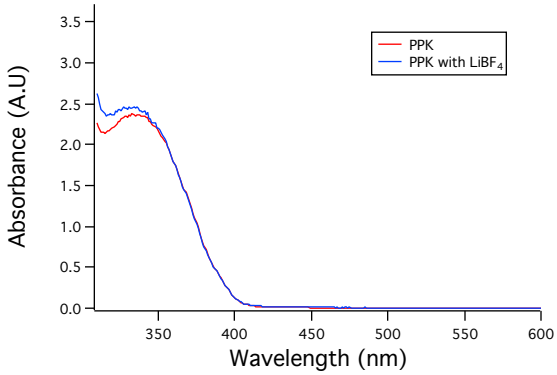

Figure 14. Absorbance spectra of PPK (**1**) and lithium coordinated PPK (**1**[a])

Selective excitation of the photosensitizer was essential in order to avoid direct excitation of other substrates. To choose an appropriate excitation wavelength, the absorption properties of the organic substrates were investigated. The absorption spectra in Figure 14 indicates that both PPK and lithium coordinated PPK do not absorb light at wavelength greater than 400 nm. The other organic substrate, MVK and lithium coordinated MVK also do not show absorption band at wavelength greater than 400 nm. With this result in mind, a xenon lamp with 400 nm longpass filter was used to irradiate the reaction mixture in order to avoid the uncontrollable reactivity that would result from the excited organic substrates.

Table 1. Negative control reactions

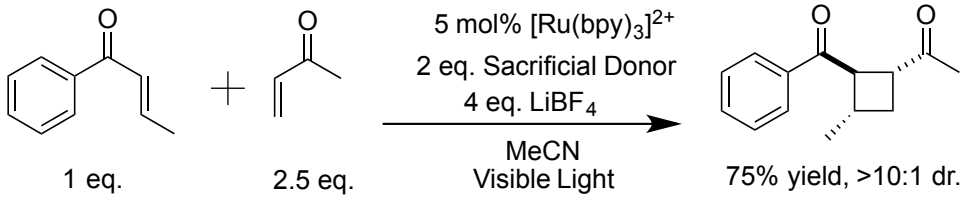

1 **2** **3**

Reaction	Photosensitizer	Donor	Product	Solvent	Yield %
1	$[Ru(bpy)_3]^{2+}$	DIPEA	Yes	MeCN	75
2	$[Ru(bpy)_3]^{2+}$	DMT	No	MeCN	0
3	$[Ru(bpy)_3]^{2+}$	TEA	Yes	MeCN	15.4
4	*fac*-$Ir(ppy)_3$	DIPEA	Yes	MeCN	60
5	*fac*-$Ir(ppy)_3$	DMT	No	MeCN	0
6	$[Cu(dsbp)_2]^{+}$	DIPEA	No	MeCN	0
7	$[Cu(dsbp)_2]^{+}$	DMT	No	MeCN	0

The exemplar reaction (Table 1, Entry 1) under our experimental conditions yielded 75% of **3** (d.r > 10:1). The yield was similar with Yoon's result, which was 81 %.[9] When DMT is used to replace DIPEA (Table 1, Entry 2), **3** was not observed. Instead, the starting material (**1**) was not consumed during the reaction and remained detectable in the ^{1}H NMR spectrum of the crude reaction mixture with new peaks from dimerized DMT (Figure 15 D). Another sacrificial electron donor, TEA, was also tested. TEA has a faster quenching rate constant (1.2×10^8 $M^{-1}s^{-1}$) than DIPEA (7.8×10^6 $M^{-1}s^{-1}$).[24] Such a reaction with better reductive quencher typically results a more efficient photochemical reaction. However, as shown in Table 1, the yield from TEA (15.4%) was significantly lower than that of DIPEA (75%). This suggests that the reaction was not following a typical reductive photocatalytic cycle.

This observation was supported by reactions utilizing alternative photosensitizers that are stronger reducing agents than $[Ru(bpy)_3]^{+}$, which has the reduction potential of – 1.70 V vs $Fc^{+/0}$. *fac*-$Ir(ppy)_3$ and $[Cu(dsbp)_2]^{+}$ were tested since reduced $[Ir(ppy)_3]^{-}$ has reduction potential of – 2.60 V vs $Fc^{+/0}$ and excited $[Cu(dsbp)_2]^{+*}$ has an oxidation potential of – 2.19 V vs $Fc^{+/0}$.[15,16] Since they are stronger reducing agents, the alternative photosensitizers should reduce organic substrates more efficiently than $[Ru(bpy)_3]^{+}$. When *fac*-$Ir(ppy)_3$ was used with DIPEA as the quencher (Table 1, Entry 4), **3** was observed with a yield of 60%. On the other hand, when *fac*-$Ir(ppy)_3$ was used with DMT (Table 1, Entry 5), the formation of **3**

was still not observed with starting substrate (**1**) remaining unconsumed. $[Cu(dsbp)_2]^+$ was also tested since the strong oxidation potential of its excited state should reduce **1** or **1**[a] directly. However, reactions using this copper photosensitizer did not form **3** in the presence of either DIPEA or DMT (Table 1, Entry 3, 6, 7). Therefore these control experiments supported our suspicion that the reaction is not following a standard reductive photocatalytic cycle.

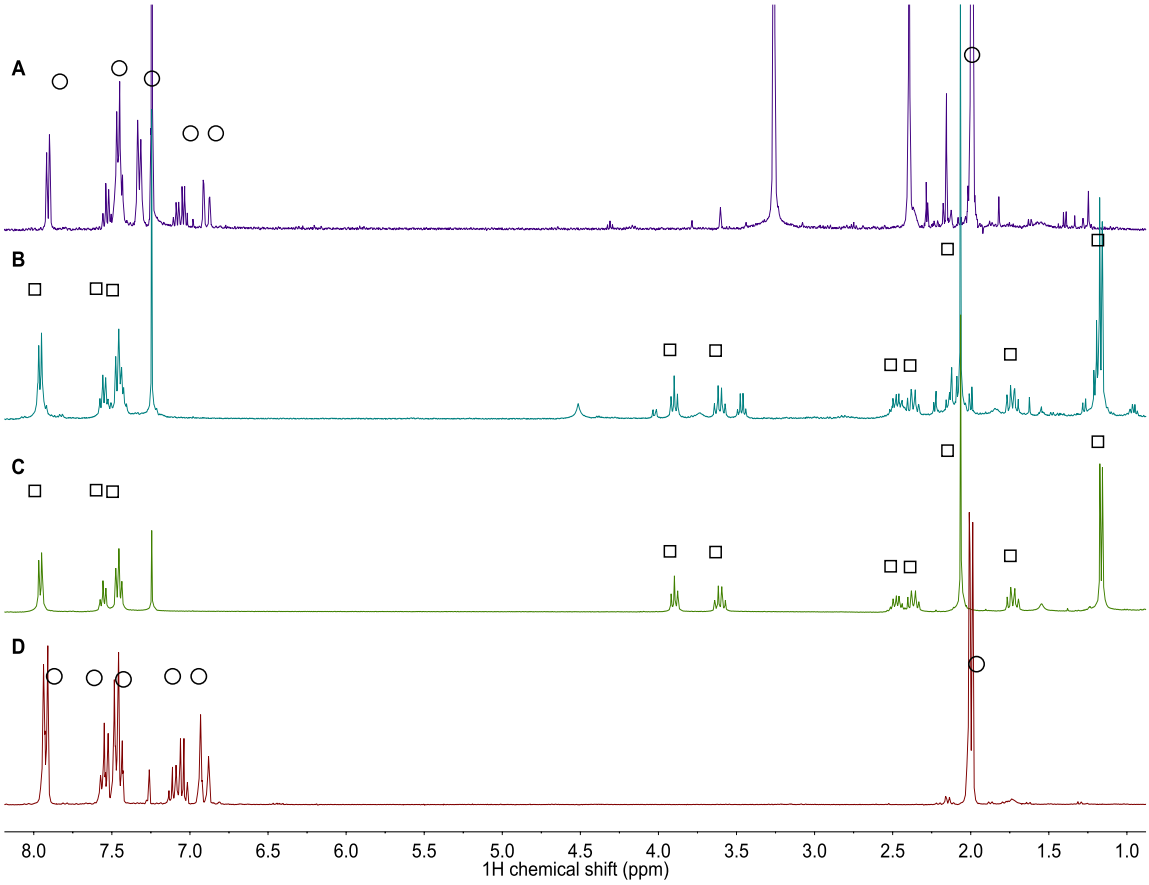

Figure 15. ^{1}H NMR spectra ($CDCl_3$, 400 MHz) of the reaction crude A: reaction with DMT, B: reaction with DIPEA, C: **3**, D: **1**. (□: peaks of **3**, O: peaks of **1**)

From these results, we observed that **3** was only observed when a trialkylamine was used as the sacrificial electron donor. When DMT was used as a sacrificial electron donor, the reaction did not generate **3** and no starting material (**1**) was consumed. The observation of starting material (**1**) demonstrated that the reduced photosensitizer cannot reduce or deliver

electron to **1**[a]. We can conclude that the standard photoredox model is not applicable to this [2+2] cycloaddition of enones.

2. Investigations of Electron Transfer Pathways

Light is an essential component as shown by control experiments, such as light-dark experiment.[22] However, inability to observe the cyclized products in the absence of trialkylamines supported our initial suspicion that this photo-driven [2+2] cycloaddition of intermolecular enones was not initiated directly by reduced photosensitizer. To correctly assign the role of the light and that of the trialkylamine, we needed to follow the proposed electron transfer pathways using Stern-Volmer kinetics, electrochemistry and flash-quench method.

2.1 Quenching Rate Determination: Stern-Volmer Kinetics

Stern-Volmer kinetics describes how efficient the quenching process occurs between a photoexcited sensitizer and a quencher.[59,60] Quenching of an excited sensitizer can be classified into dynamic quenching and static quenching. Dynamic quenching, also known as collisional quenching, occurs when photoexcited sensitizer is deactivated by collision with the quencher. The resulting deactivation decreases the intensity of luminescence (Figure 16a). In dynamic quenching, both sensitizer and quencher are not chemically altered. The decreased in the intensity of luminescence upon quenching can be described by equation 1,

$$\frac{\Phi_0}{\Phi} = \frac{\tau_0}{\tau} = 1 + K_{sv}[Q] \qquad (1)$$

$$K_{sv} = k_q \tau_0 \qquad (2)$$

where ϕ_0 is the luminescence quantum yield in absence of quencher, and ϕ is luminescence quantum yield with quenchers. K_{sv} is the Stern-Volmer constant, k_q is bimolecular quenching rate constant, [Q] is concentration of quencher, and τ_0 is the lifetime of photoexcited sensitizer in the absence of quencher. The term ϕ_0/ϕ, or τ_0/τ is linearly dependent on the concentration of quencher [Q] with y-intercept of 1. Its slope represents K_{sv} (Figure 16b).

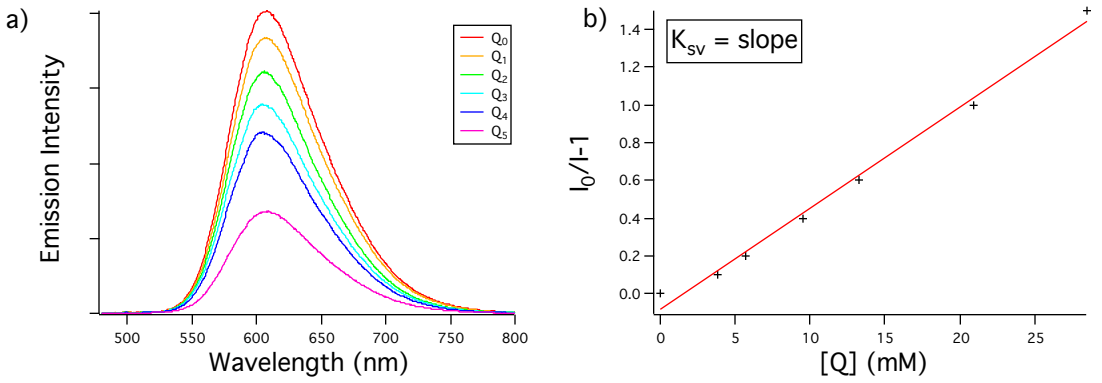

Figure 16. a) A typical steady-state photoluminescence quenching experiment; b) the corresponding Stern-Volmer plot

Unlike dynamic quenching, static quenching forms a non-fluorescent exciplex between quencher and sensitizer in the ground state. When this non-fluorescent exciplex absorbs light, it dissociates without emitting a photon, resulting the decrease in luminescence. Thus, quenching rate constant, which is calculated from based on decreased intensity of luminescence, would be inadequate. However, measuring lifetime of the excited sensitizer provides the lifetime of uncomplexed sensitizer, since this fraction is not impeded by non-fluorescent exciplex. Therefore, in static quenching, a lifetime study is used to find K_{sv}, where $\frac{\tau_0}{\tau} = 1 + K_{sv}[Q]$.[59,60]

To verify the first electron step, the Stern-Volmer experiment was performed to see whether any of the substrates present in the reaction (**1**, **2**, **1**$^{\mathbf{a}}$, **2**$^{\mathbf{a}}$, and $LiBF_4$) can quench the photoexcited $[Ru(bpy)_3]^{2+*}$ (Figure 17). For the Stern-Volmer experiment with **1**$^{\mathbf{a}}$ and **2**$^{\mathbf{a}}$, a 1:1 equivalent of organic substrate (either **1** or **2**) and $LiBF_4$ was prepared as a quencher solution. The sacrificial electron donors (DIPEA, TEA, and DMT) were reported to have sufficient electron transfer rates with excited $[Ru(bpy)_3]^{2+*}$, while the quenching between $[Ru(bpy)_3]^{2+*}$ and $LiBF_4$ does not occur.[22,41,58]

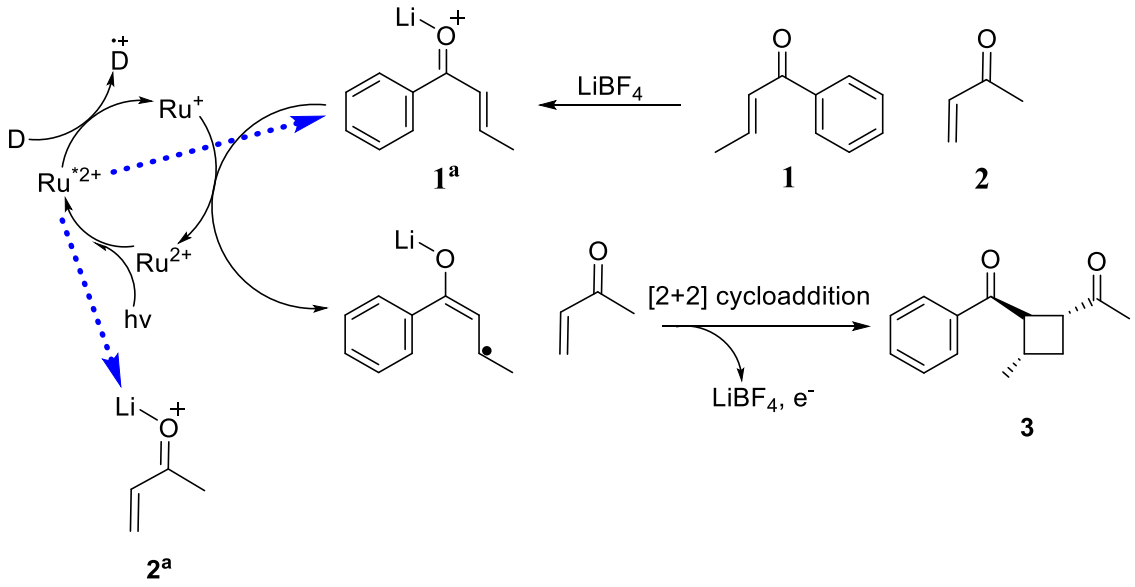

Figure 17. Possible quenching pathways between substrates and excited $[Ru(bpy)_3]^{2+*}$ (**1**: Phenyl 1-propenyl ketone, **2**: Methyl vinyl ketone, **1**^{a}: lithium coordinated **1**, **2**^{a}: lithium coordinated **2**)

Table 2. K_{sv} and k_q between $[Ru(bpy)_3]^{2+*}$ and organic substrates (**1**, **2**, **1**^{a}, and **2**^{a}), and reported k_q of sacrificial electron donors (DIPEA, TEA, and DMT)

Quencher	K_{sv} (M^{-1})	k_q($M^{-1}s^{-1}$)	Quenching
1	Not-measurable (too low)		No
2	Not-measurable (too low)		No
1^{a}	1.57 (too low, non-linear)		No
2^{a}	0.71 (too low)		No

As shown in Table 2 and Figure S4, none of the substrates quench excited $[Ru(bpy)_3]^{2+*}$, while sacrificial electron donors (DIPEA, TEA, and DMT) had sufficient quenching rate constants (7.8×10^{6} $M^{-1}s^{-1}$, 1.2×10^{8} $M^{-1}s^{-1}$, 1.5×10^{9} $M^{-1}s^{-1}$ respectively).[22,41,61] K_{sv} from **1**^{a} and **2**^{a} are too low to be considered as quenching activities. Consequently with no quenching of static photoluminescence (or PL lifetime) of excited $[Ru(bpy)_3]^{2+*}$ upon varying the concentration of **1**^{a}, **2**^{a}, or $LiBF_4$ we conclude that the electron transfer between

excited photosensitizer to organic substrates (**1**, **2**, **1**^{a}, and **2**^{a}) is inefficient. This observation supports the first electron transfer step of the mechanism, shown in Figure 12.[9]

2.2 Electrochemistry

In order to determine the ground state energies of target organic substrates (**1**, **2**, **1**^{a}, and **2**^{a}) and reduced photosensitizer, cyclic voltammetry was performed. The electrochemistry in acetonitrile exhibited unusual behavior that electrochemical reduction of **1**^{a} degrades, presumably due to electrode fouling. The unexpected behavior made quantified measurements of this reduction peak be impossible. Due to the unusual behavior between $LiBF_4$ and **1** in acetonitrile, DMF was used to observe the effect of the addition of Lewis acid to the electrochemical reduction of peak. Reduction of both organic substrates (**1** and **2**) exhibited irreversible peaks. On the other hand, oxidation of $[Ru(bpy)_3]^+$ exhibited a reversible peak.

Table 3. Reduction potentials of organic substrates (**1**, **2**, **1**^{a}, and **2**^{a}) and oxidation potential of $[Ru(bpy)_3]^+$ in DMF with 0.1M $TBABF_4$ as electrolyte.

	Redox potential (vs $Fc^{+/0}$) in DMF	
$[Ru(bpy)_3]^+$	- 1.74 V	
Ketone	Without $LiBF_4$	With $LiBF_4$
Phenyl 1- propenyl ketone (**1**)	- 2.31 V	- 2.08 V (**1**^{a})
Methyl vinyl ketone (**2**)	- 2.54 V	- 2.31 V (**2**^{a})

*Cyclic Voltammograms are on Figure S10 – S12.

As shown in Figure 18, **1** has a reduction peak at – 2.31 V vs $Fc^{+/0}$. The reduction potential of **2** was determined to be – 2.54 V vs $Fc^{+/0}$. The addition of $LiBF_4$ lowered the reduction potential of both ketones **1** and **2** by 230 mv. The resulting reduction potential of **1**^{a} was – 2.08 V vs $Fc^{+/0}$, while **2**^{a} was – 2.31 V vs $Fc^{+/0}$. To qualitatively compare the redox potential between organic substrates and reduced photosensitizer, cyclic voltammetry of $[Ru(bpy)_3]^+$ was performed and its oxidation potential was determined to be – 1.74 V vs $Fc^{+/0}$.

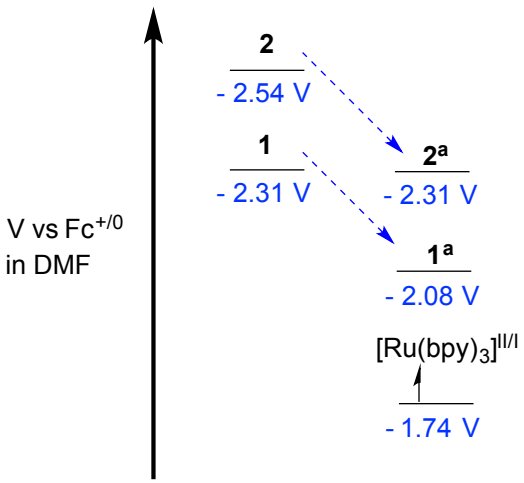

Figure 18. Energy scheme of organic substrates (**1**, **2**, **1**^{a}, and **2**^{a}) and $[Ru(bpy)_3]^+$; (blue arrow indicates the decreasing of reduction potential upon addition of $LiBF_4$

The reduction potential of aryl enone (**1**), – 2.31 V, was lower than that of aliphatic enone (**2**), – 2.54 V (Table 3). The addition of Lewis acid, $LiBF_4$, lowered the reduction potential by 230 mV for both enones. This indicated that under the described reaction conditions, **1**^{a} is the species that will accept the electron from a reducing agent. As shown in Figure 18, the energy of ground state of **1**^{a} located 0.34 V above the oxidation potential of $[Ru(bpy)_3]^+$, which does not favor electron transfer from $[Ru(bpy)_3]^+$ to **1**^{a}.

2.3 Flash-Quench Experiments

The properties of photosensitizers in the reduced (or oxidized) state (referred to as radical anion or radical cation), such as absorption spectrum, redox potential, and electron transfer capability, are quite different from the properties of the photosensitizers in the corresponding ground and/or excited states. The reduced/oxidized photosensitizer exists as reactive ionized radical species, which is difficult to isolate as a stable compound. As a result, the characterization of their physical and chemical properties becomes non-trivial. To overcome such problems, a flash-quench experiment (Figure 19) was chosen to characterize the reduced/oxidized substrates in terms of their absorption, lifetime, and electron transfer properties.[62–66]

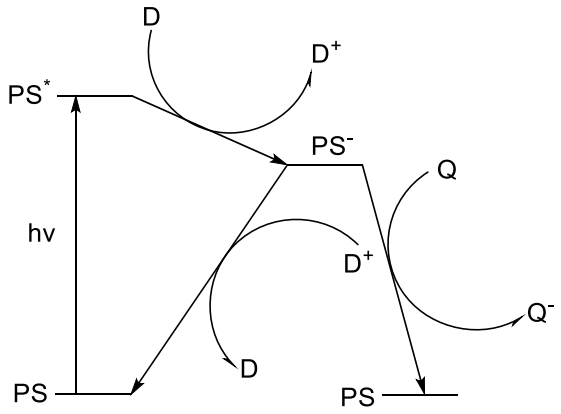

Figure 19. Qualitative flash-quench energy diagram (PS: photosensitizer, D: donor, D^+: oxidized donor, Q: quencher, Q^-: reduced quencher)

Figure 19 represents the series of electron transfer processes that involved in a flash-quench experiment. Flash photolysis of photosensitizer with an excess amount of sacrificial electron donor (D) generates quantitative amount of reduced photosensitizer (PS^-). This reduced species returns back to its ground state (PS) either through bimolecular charge recombination with oxidized donor (D^+) or by electron transfer to a quencher (Q).[62–66] Using transient absorption spectroscopy, the electron transfer rate (k_{et}) between the reduced photosensitizer and quencher can be calculated by plotting quencher concentration and the k_{obs} of the reduced photosensitizer.

With flash quench-method, the 2nd electron transfer step between reduced photosensitizer and organic substrate can be investigated. In this project, $[Ru(bpy)_3]^{2+}$ was used as a photosensitizer with DMT as sacrificial electron donor. In the presence of excess DMT, the reduced $[Ru(bpy)_3]^+$ radical anion was formed under 452 nm excitation. The lifetime of $[Ru(bpy)_3]^+$, which has max absorbance at 505 nm, was measured by nanosecond transient absorption spectroscopy.[63–65,67,68] Addition of various concentration of quencher (**1**[a] and **2**[a]**)** to flash-quench mixture followed by excitation at 452 nm was performed to observe the decay rate of $[Ru(bpy)_3]^+$ species.

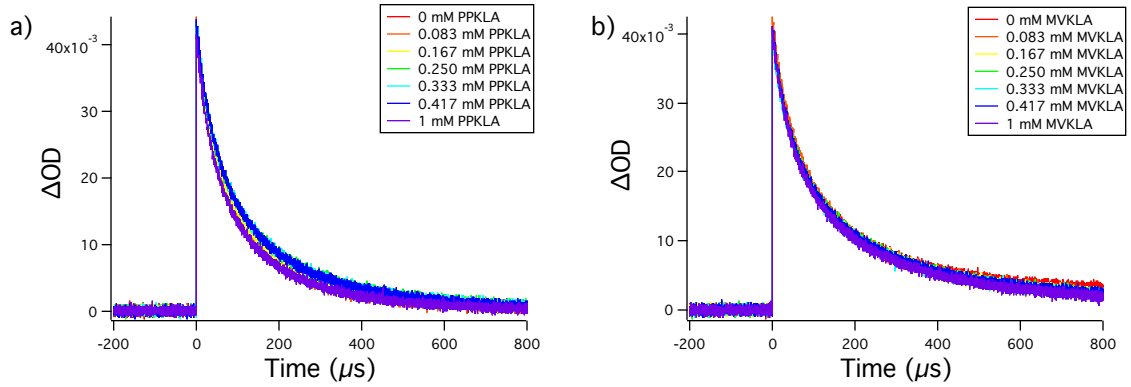

Figure 20. Transient absorption decays of $[Ru(bpy)_3]^+$ monitored at 505 nm. Conditions: $[Ru(bpy)_3]^{2+}$ (2.5×10^5 M), DMT (0.3 M), and with quenchers (a) PPKLA: **1**[a], b) MVKLA: **2**[a]), excitation wavelength: 452 nm.

According to the proposed mechanism, **2**[a] was projected to show no quenching, while quenching by **1**[a] was expected. However, as shown in Figure 20, the addition of organic substrates (**1**[a] and **2**[a]) could not quench $[Ru(bpy)_3]^+$. The inability to quench $[Ru(bpy)_3]^+$ indicates that 2[nd] electron transfer step, electron transfer from $[Ru(bpy)_3]^+$ to **1**[a], does not occur. Along with the electrochemical data, this confirms that electron transfer from $[Ru(bpy)_3]^+$ to **1**[a] is not the mechanism for formation of the products.

3. Amine Radical Intermediates

3.1 Steady-State Absorption Study

The flash-quench experiment with DIPEA as sacrificial electron donor was also performed, but the experiment could not detect the transient absorption decay of $[Ru(bpy)]^{+}$. We assumed that this was caused by a secondary reduction of photosensitizer by trialkylamine radical cation.[34] The secondary reduction by amine radical cation causes permanent spectral changes. To verify our understanding on the immeasurable decay kinetics with DIPEA, the steady-state absorption study was performed using HeCd laser as an excitation source (442 nm). Two solutions with different sacrificial electron donors were prepared. As shown in Figure 21, the steady-state absorption spectra were taken with intervals of 5 minutes to monitor any induced spectral changes.

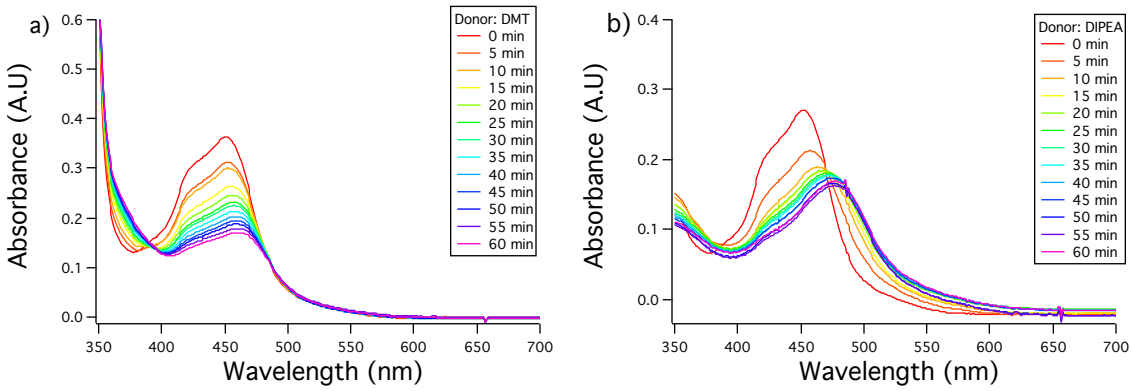

Figure 21. The reaction of $[Ru(bpy)_3]^{2+}$ (2.5×10^{-5} M) with DMT (a) or DIPEA (b) in acetonitrile monitored by steady-state absorption spectroscopy. The concentration of donor was 0.3 M. The excitation wavelength was 442 nm.

As shown in Figure 21, prolonged irradiation of a $[Ru(bpy)_3]^{2+}$ solution with DMT resulted in the gradual disappearance of the MLCT absorption band without significant spectral shifts. On the other hand, the use of DIPEA resulted in the permanent bathochromic shift of the absorption spectra of $[Ru(bpy)_3]^{2+}$. The resulting spectra resembled the absorption spectrum of $[Ru(bpy)_3]^{+}$ radical anion.[69] Upon the exposure to H_2O or O_2, the shifted spectra reverted back to the original spectra. This observation was consistent with the aspects of secondary reduction of photosensitizer by amine radical cation, which has been reported by

Whitten.[34] The mechanism of secondary photosensitizer reduction state involves an α-amino radical, which is capable of reducing ground state photosensitizer to generate $[Ru(bpy)_3]^+$. Consequently, the permanent spectral changes observed in solution with DIPEA suggest the presence of a photogenerated secondary reducing agent, most likely an α-amino radical.

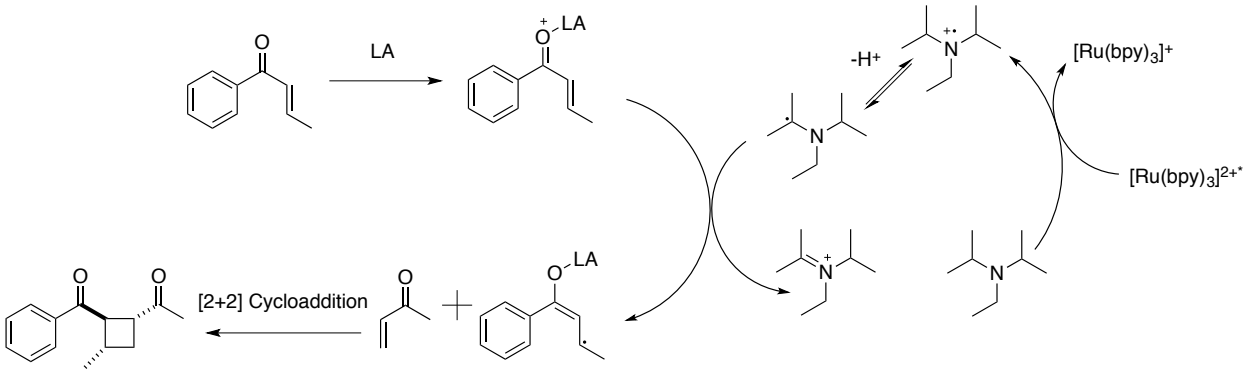

Figure 22. Newly proposed mechanism that involves α–amino radical

Based on the investigation of electron transfer pathways and steady-state absorption, we conclude that the reduced photosensitizer does not reduce the organic substrate. The presence of an α-amino radical and its role as a reducing agent inspire us to propose a new mechanism as shown in Figure 22. Here, a photogenerated α-amino radical is the active reducing agent for the lithium coordinated aryl enone initiating [2+2] cycloaddition. The role of the photosensitizer is to generate an amine radical cation, which transforms into an α-amino radical.

3.2 Characterization of α–amino Radical of DIPEA

Since, α–amino radical can be a reducing agent to potentially reduce **1**[a] to initiate [2+2] cycloaddition, characterization of α–amino radicals is needed to define the role of such α–amino radicals in [2+2] cycloaddition reactions. Unfortunately, α–amino radicals are unstable compound and cannot be isolated. Thus, the characterization of α–amino radical was solely depended on its cyclic voltammetry.

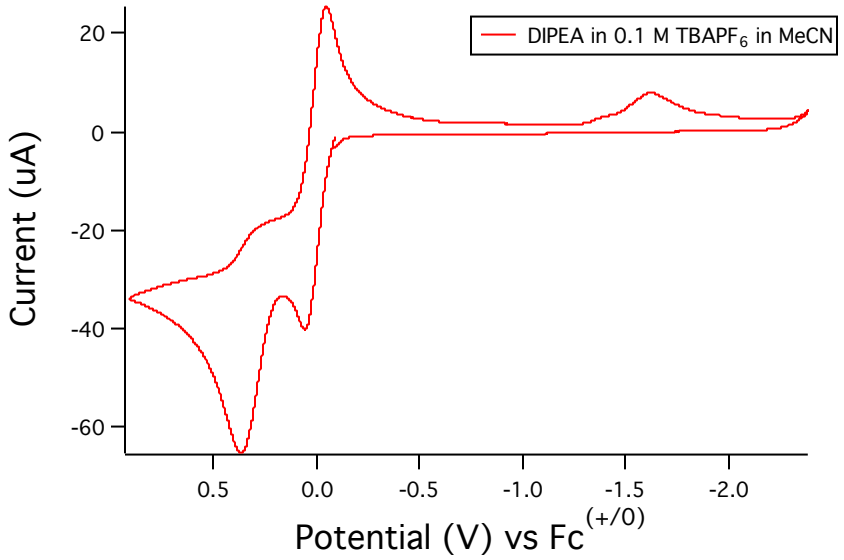

Figure 23. Cyclic Voltammetry of the DIPEA

As shown in Figure 23, oxidation of DIPEA occurs at 0.32 V vs $Fc^{+/0}$, which results in the formation of a trialkylamine radical cation. Thus, a trialkylamine radical undergoes secondary oxidation at – 1.62 V vs $Fc^{+/0}$, producing an iminium ion. This second oxidation peak only appears when the voltammogram is swept from positive to negative voltage. In the case of a reverse sweep from negative voltage to positive voltage, this oxidation peak was not present. This indicates that the second oxidation peak is a distinct character of the α–amino radical. In addition, the peak intensity of the 2nd oxidation peak is relatively smaller than that of 1st oxidation peak. Considering that α–amino radicals are formed through an equilibrium with the trialkylamine radical cation, the α–amino radical should be present in lower concentrations than amine radical cation.[32]

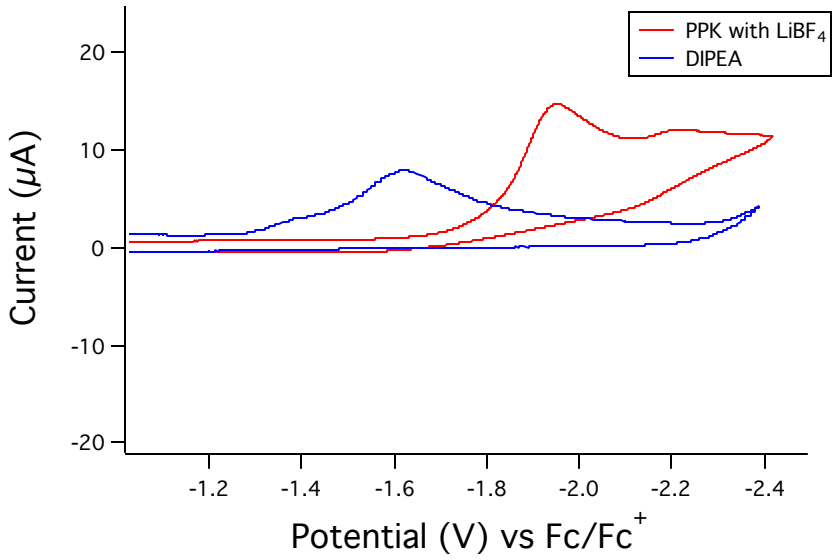

Figure 24. Cyclic Voltammetry of **1**[a] and α–amino radical of DIPEA

After the characterizing the α–amino radical, we compared the oxidation potential of α–amino radical to the reduction potential of **1**[a] in acetonitrile. The reduction of **1**[a] in acetonitrile occurred at – 1.95 V vs $Fc^{+/0}$, while the oxidation of α–amino radical occurred at – 1.62 V vs $Fc^{+/0}$. Typically, the 330 mV difference of potential is energetically unfavorable an electron transfer process. Despite their unmatched potentials, the 2nd oxidation peak partially overlapped with the reduction peak of the **1**[a] as shown in figure 24. The overlapping potentials between two species indicate that the electron transfer process is possible, even though electrochemical data is not conclusive evidence of an electron transfer processes between α–amino radical and **1**[a].

We also investigated the oxidation potential of TEA. Its 2nd oxidation occurs at – 1.52 vs $Fc^{+/0}$ (In case of α–amino radical of DIPEA was – 1.62 V vs $Fc^{+/0}$).[34] The 2nd oxidation peak of TEA indicates that the α–amino radical of TEA is less reducing than that of DIPEA. This is consistent with our observations on control experiments that TEA yields less **3** than when DIPEA is used. The comparison of the oxidation potential of the α–amino radical and yield efficiencies of DIPEA and TEA allowed to conclude that the reaction is directly proportional to the reducing power of α–amino radical of amine. Such observation strengthens the argument that the [2+2] cycloaddition of enones is initiated by a photogenerated α–amino radical.

3.3 Generation of amine radical cation via the reaction between $[Ru(bpy)_3]^{3+}$ and DIPEA

With potential evidence that an α–amino radical initializes the reaction, we attempted to chemically generate α–amino radicals to initiate the reaction. However, because of the unstable nature of α–amino radicals, we decided to generate an amine radical cation, which is in equilibrium with α–amino radical.[32] One method that would allow us to generate an amine radical cation is using $[Ru(bpy)_3]^{3+}$ as a one electron oxidant. After examining the redox properties of $[Ru(bpy)_3]^{3+}$ (0.88 V vs $Fc^{+/0}$) and DIPEA (0.34V vs $Fc^{+/0}$), we concluded that an amine radical cation should be generated through the reaction of $[Ru(bpy)_3]^{3+}$ and trialkylamine.[15,70]

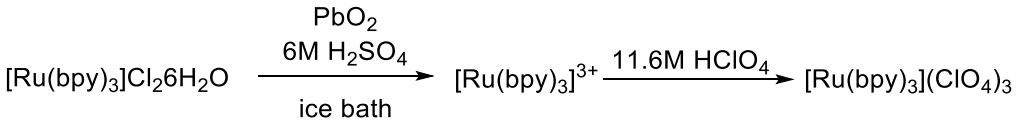

Figure 25. The synthesis of $[Ru(bpy)_3](ClO_4)_3$.

$[Ru(bpy)_3]^{3+}$ can be generated upon addition of oxidant, PbO_2, with sulfuric acid at 0 °C. When oxidant was added into a $[Ru(bpy)_3]^{2+}$ solution, the color of the solution changes from orange to dark green, which is distinct to $[Ru(bpy)_3]^{3+}$.[71–75] $[Ru(bpy)_3]^{3+}$ can be isolated as a stable compound with suitable counter ions, such as $[PF_6]^-$ or $[ClO_4]^-$.[71–75] $[Ru(bpy)_3](ClO_4)_3$ was chosen due to its superior stability relative to $[Ru(bpy)_3](PF_6)_3$.[71,72,76]

In a glovebox without light, the solution of $[Ru(bpy)_3](ClO_4)_3$ was added into the reaction mixture, which contained the organic substrates (**1**, **2**, $LiBF_4$, and DIPEA). As shown in Figure 26, the ^1H NMR spectrum of the reaction crude did not show any characteristic peaks of **3**. Failure to generate **3** with amine radical cation could indicate that the reaction is not initiated by amine radical cations. However, chemiluminescence was observed during reaction, allowing for an alternative conclusion to be reached.

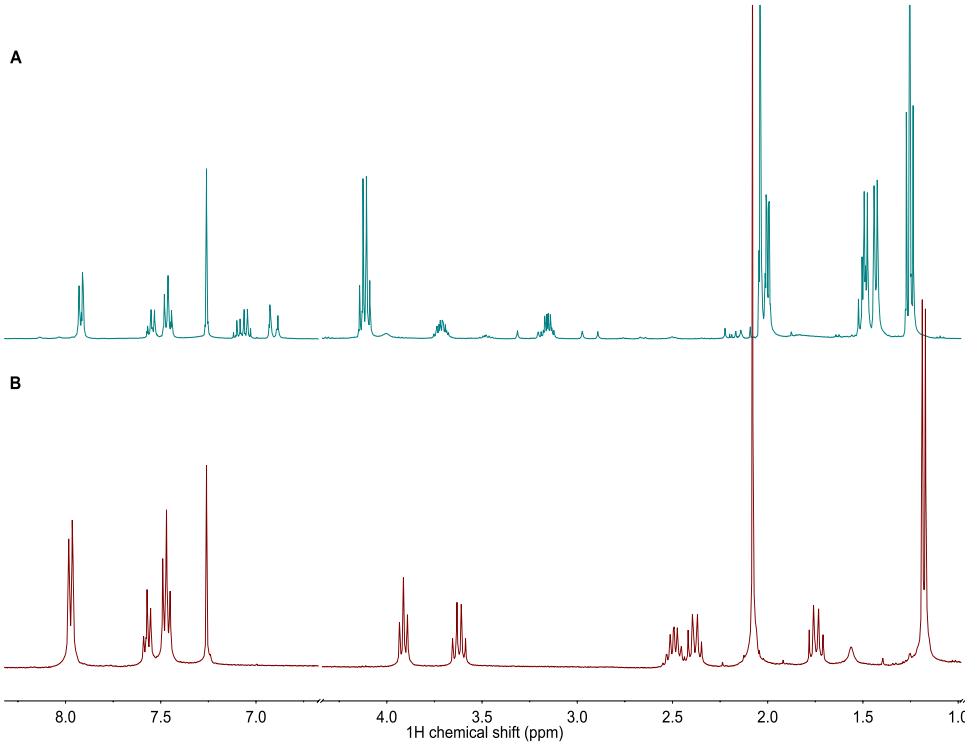

Figure 26. The comparison of ^{1}H NMR spectra ($CDCl_3$, 400 MHz): A: organic crude under negative control reaction with $[Ru(bpy)_3]^{3+}$ and DIPEA; B: **3**

Initially, the appearance of chemiluminescence was assumed to be evidences for amine radical cation generation.[70] However, failure to produce the product raised a question of whether the resulting intermediate between $[Ru(bpy)_3]^{3+}$ and DIPEA was indeed an amine radical cation or some other intermediate. Amine radical cation from simple aliphatic amines are known to be very reactive transforming into iminium ion rapidly in polar solvents.[33] Furthermore, a chemiluminescence mechanism was known to produce iminium ions as the final amine product. As demonstrated in Figure 27, amine radical cation can rapidly lose hydrogen, and form α–amino radical.[32,77–79] In turn, α–amino radical can reduce the ground state of $[Ru(bpy)_3]^{2+}$ to form $[Ru(bpy)_3]^{+}$. As $[Ru(bpy)_3]^{+}$ and $[Ru(bpy)_3]^{3+}$ recombine, the single electron transfer step happens with the generation of excited $[Ru(bpy)_3]^{2+*}$, which produces chemiluminescence. At the same time, oxidation of α–amino radical results in the formation of iminium ions.[70,77,79]

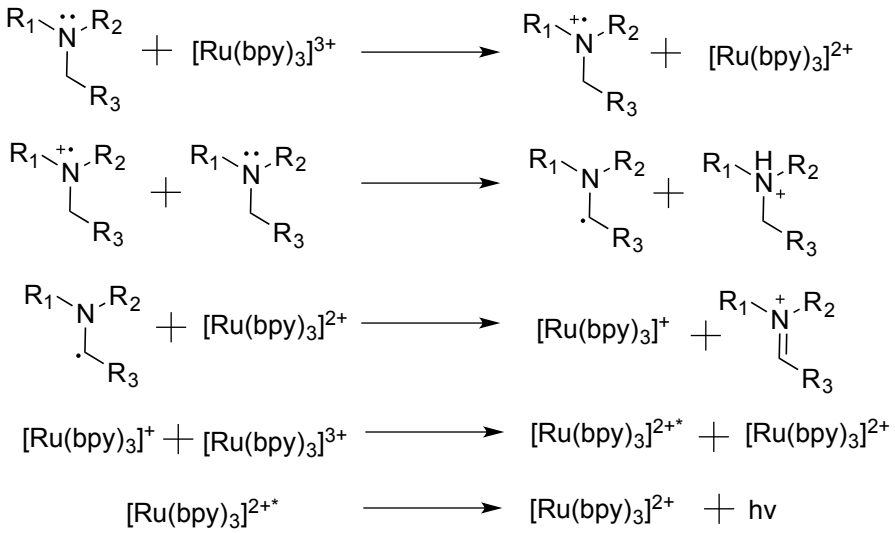

Figure 27. Chemiluminescence mechanism

The combination of $[Ru(bpy)_3]^{3+}$ and DIPEA quickly produced the iminium ion as a final intermediate. As a consequence, organic substrates (**1**, **2**, **1**[a], and **2**[a]) were unable to kinetically react with amine radical cation or α-amino radical. Despite the failure to access appropriate concentration of amine radical cation, the iminium ion was present and could potentially react with the organic substrates (**1**[a] and **2**[a]). However, no conversion of **1** was observed, which indicates that the reaction between the iminium ion and organic substrates does not occur. Consequently, the inability to form **3** eliminates one possible reaction pathway that involves an iminium ion.

PART III: Conclusion

The current widely accepted mechanism of many photo-driven catalytic reactions claims that the reduced photosensitizer reduces the organic substrates to initiate the reaction. Unfortunately, only handfuls of mechanistic investigations have been reported on the reductive quenching process of photoredox catalysis.[22–25] The mechanistic details of photoredox catalysis limit often researchers the empirical improvements, rather than rational improvements. Here, we have demonstrated an inconsistency when the electron transfer processes in photo-driven [2+2] cycloaddition of enones in the proposed mechanism and our observations. A control reaction with 4-*N,N*-dimethylaminotoluene (DMT), a chemically inert reductive quencher, shows that the reaction cannot proceed in absence of trialkylamine. To fully verify the effect of trialkylamines in photoredox catalysis, each of the electron transfer processes can be investigated with Stern – Volmer kinetics and a flash quench method.

Control reactions with DMT as an alternative sacrificial electron donor do not produce **3**. Meanwhile, the reaction with trialkylamine produced **3**. The first electron transfer step, where a sacrificial electron donor quenches an excited photosensitizer, was verified by Stern-Volmer kinetics. With the exception of known sacrificial electron donors, all other organic substrates (**1**, **2**, $\mathbf{1^a}$, and $\mathbf{2^a}$) exhibited no quenching of the photoexcited $[Ru(bpy)_3]^{2+*}$. In the case of the second electron transfer step, the results from flash-quench experiment and electrochemistry are not consistent with the proposed mechanism, which proposed reduction of $\mathbf{1^a}$ by $[Ru(bpy)_3]^{+}$ to initiate the [2+2] cycloaddition. The 340 mV difference between reduction potential of $\mathbf{1^a}$ and oxidation potential of $[Ru(bpy)_3]^{+}$ suggested that the electron transfer process was thermodynamically unfavorable. This step was further explored with a flash-quench experiment that showed no quenching of $[Ru(bpy)_3]^{+}$ by either $\mathbf{1^a}$ or $\mathbf{2^a}$. Inconsistency of electron transfer mechanism and inability to form a product with DMT indicates that the reactivity of amine radical cations needs to be investigated.

These inconsistencies drove us to focus on the formation of one of the reactive trialkylamine radical intermediates, α–amino radical. Due to its unstable nature, only electrochemical characterization of α–amino radical was performed. The resulting oxidation opens up the potential electron transfer process, since the oxidation of α–amino radical

partially overlaps the reduction potential of **1**[a]. Based on this observation of a potential electron transfer process, we attempted to chemically generate α–amino radical through the reaction between $[Ru(bpy)_3]^{3+}$ and DIPEA. Unfortunately, the α-amino radical was not accessible due to a fast chemiluminescence process, which forms iminium ions and prevents the formation of **3**.

Due to the limitation on accessing the α-amino radical as a stable form, the mechanism of the reaction was not fully characterized. The direct evidence, which α-amino radical is initiating the reaction, was unavailable. However, considering the observation from control experiments and electron transfer investigations, we still believe that an α-amino radical initiates the [2+2] cycloaddition by reducing **1**[a], in contrast to the previously proposed mechanisms, where $[Ru(bpy)_3]^{+}$ acts as the only reducing agent.

Experimental

General

All chemicals were used as received unless otherwise noted. $Ru(bpy)_3Cl_2 \cdot 6H_2O$, $LiBF_4$, *N*-ethyldiisopropylamine, DMT, and TEA were purchased from Acros Organics. Phenyl 1-propenyl ketone was purchased from TCI, and purified by column chromatography prior to use. Methyl vinyl ketone was purchased from Alfa Aesar and purified by distillation. 4-*N,N*-dimethylaminotoluene was purchased from Sigma-Aldrich. $LiBF_4$ was purchased from Strem Chemical Company. *N*-ethyldiisopropylamine was purchased from Alfa Aesar. For all photochemical reactions, dry glassware was used.

Synthesis of 1-((1R,2R,3S)-2-Benzoyl-3-methylcyclobutyl)ethan-1-one :

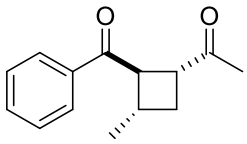

In a 25 ml round bottom flask, 25.0 mg (0.03 mmol) of $Ru(bpy)_3Cl_2 \cdot 6H_2O$, 100 mg (0.69 mmol) of phenyl 1-propenyl ketone, 140 µl of (1.68 mmol) methyl vinyl ketone, and 0.2610 g (2.78 mmol) of $LiBF_4$ was dissolved in ~10ml of dry acetonitrile. Then 240 µl (1.37 mmol) of diisopropylethylamine was added. Once diisopropylethylamine was added, the reaction mixture was deoxygenated via freeze-pump-thaw three times and kept under N_2. The mixture was irradiated with Xenon lamp (160W) with a 400 nm longpass filter for 4 hours. The solvent was then removed under reduced pressure. The crude reaction mixture was purified by column chromatography. (hexane: EtOAc = 6:1). ^{1}H NMR (400 MHz, $CDCl_3$): δ 7.98 (dt, J = 7.2Hz, 1.6Hz, 2H), 7.57 (tt, J = 7.6 Hz, 1.6 Hz, 1H), 7.47 (dt, J = 7.6 Hz, 2H), 3.91 (t, J = 8.4 Hz, 1H), 3.62 (q, J = 9 Hz, 1H), 2.49 (m, 1H), 2.38 (m, 1H), 2.08 (s, 3H), 1.75 (q, J = 9.3 Hz, 1H), 1.18 (d, J = 8 Hz, 3H) ^{13}C NMR (100 MHz, $CDCl_3$): 208.4, 199.5, 136.2, 133.5, 128.8, 49.9, 43.6, 31.1, 29.4, 27.8, 21.1; Yield: 110mg (74%).

General photoreaction procedure:

In a 25ml round bottom, 5 mol. % of photosensitizer, and 2.8 eq. $LiBF_4$ were dissolved in ~10 ml of dry acetonitrile. 1 eq. of phenyl 1-propenyl ketone, 2.4 eq. of methyl vinyl ketone, and 2 eq. of sacrificial electron donors were then added into solution. The

reaction flask was deoxygenated via freeze-pump-thaw and backfilled with N_2 gas. The mixture was irradiated with Xenon lamp (160W) using an appropriate longpass filter. The reaction was allowed to proceed for 4 hours. After 4 hours, the solvent was removed under reduced pressure. The mixture was examined by using ^{1}H NMR (400 MHz) in $CDCl_3$.

Synthesis of $Ru(bpy)_3(ClO_4)_3$

60 mg of $Ru(bpy)_3Cl_2 \cdot 6H_2O$ were dissolved in ~2 ml of 0.6M H_2SO_4. A scoop of PbO_2 was added with stirring. The orange solution turned into dark green solution. The solution was stirred for an additional 30 minutes to 1 hour. The dark green solution was cooled in an ice bath, and then filtered by using fine-frit glass filter. The filtered solution was cooled in ice bath, and ~0.5 ml of 70 % $HClO_4$ (11.6 M) was added into solution. The addition was done by drop wisely over 10 minutes. When the green precipitate starts to form, the solution was left in ice bath for several hours to form dark green crystals. Dark green crystals were filtered with medium-size glass filter, and washed briefly with cold water. The obtained product was stored in the glove box until use.

General procedure for $[Ru(bpy)_3]^{3+}$ negative control experiments

All experiments were performed in glovebox. $LiBF_4$ (4 eq.), methyl vinyl ketone (2.4 eq.), phenyl 1-propenyl ketone (1 eq.), and DIPEA (1 eq.) was dissolved in ~1ml of dry acetonitrile. In a separate vial, $[Ru(bpy)_3](ClO_4)_3$ (1 eq.) was dissolved. Into the reactant mixture, $[Ru(bpy)_3]^{3+}$ solution was slowly added drop wise to the reactant mixture. During the addition of $[Ru(bpy)_3]^{3+}$ solution, the reaction mixture was gently swirled. After 1 hour, the reaction was assumed to be complete. The resulting mixture was examined by using ^{1}H NMR (400 MHz) in $CDCl_3$.

Physical measurements

^{1}H NMR (400 MHz) and ^{13}C NMR (100 MHz) spectra were measured on Varian Unity Inova spectrometer. All spectra was referenced to the solvent ($CDCl_3$) residual peak (7.26 ppm for ^{1}H and 77.16 ppm for ^{13}C). NMR data were analyzed using MestReNova 9.0.1

software. Steady-state emission spectra were measured on FS920 fluorescence spectrometer (Edinburgh Instrument) with 450 W Xenon lamp as excitation source. In static quenching experiments, nitrogen-pumped broadband dye laser from PTI (Gl-301 dye laser) was used. Transient kinetic absorption was measured using LP 920 Laser Flash Photolysis system (Edinburgh Instrument). The sample was excited with Vibrant 355 LD-UVM Nd:YAG/OPO system (OPOTEK). Steady-state absorption spectra were measured using Agilent 8453 diode array UV spectrophotometer. Samples were excited with He/Cd Series 74 laser from Melles-Griot at 442 nm. Experimental data were processed with Igor Pro 6.32 software.

Electrochemistry

All electrochemical measurements were performed in a glovebox using 0.1 M of $TBABF_4$ as supporting electrolyte in anhydrous DMF or anhydrous acetonitrile. Cyclic voltammetry was performed using a standard procedure in a three-electrode configuration: carbon working electrode, Pt wire counter electrode, and 0.01 M $Ag/AgNO_3$ reference electrode. Ferrocenium/ferrocene was used as an internal standard.

References

(1) Ramamurthy, V.; Corbin, D. R.; Johnston, L. J. *J. Am. Chem. Soc.* **1992**, *114*, 3870–3882.

(2) Roth, H. D. *Angew. Chemie Int. Ed. English* **1989**, *28*, 1193–1207.

(3) Balzani, V.; Credi, A.; Venturi, M. *Photochemical conversion of solar energy*; 2008; Vol. 1.

(4) Gust, D.; Moore, T. a. *Science.* **1989**, *244*, 35–41.

(5) Gust, D.; Moore, T. A.; Moore, A. L. *Acc. Chem. Res.* **1993**, *26*, 198–205.

(6) Shi, L.; Xia, W. *Chem. Soc. Rev.* **2012**, 7687–7697.

(7) Yoon, T. P. *ACS Catal.* **2013**, *3*, 895–902.

(8) Schultz, D. M.; Yoon, T. P. *Science.* **2014**, *343*, 1239176.

(9) Du, J.; Yoon, T. P. *J. Am. Chem. Soc.* **2009**, *131*, 14604–14605.

(10) Nicewicz, D. a; MacMillan, D. W. C. *Science*. **2008**, *322*, 77–80.

(11) Narayanam, J. M. R.; Tucker, J. W.; Stephenson, C. R. J. *J. Am. Chem. Soc.* **2009**, *131*, 8756–8757.

(12) Reckenthäler, M.; Griesbeck, A. G. *Adv. Synth. Catal.* **2013**, *355*, 2727–2744.

(13) Yoshimura, A.; Hoffman, M. Z.; Sun, H. *J. Photochem. Photobiol. A: Chem,* **1993**, *70*, 29–33.

(14) Prier, C. K.; Rankic, D. A.; MacMillan, D. W. C. *Chem. Rev.* **2013**, *113*, 5322–5363.

(15) Koike, T.; Akita, M. *Synlett.* **2013**, *24*, 2492–2505.

(16) Khnayzer, R. S.; Mccusker, C. E.; Olaiya, B. S.; Castellano, F. N. *J. Am. Chem. Soc.* **2013**, *135*, 14068–14070.

(17) Zeitler, K. *Angew. Chemie - Int. Ed.* **2009**, *48*, 9785–9789.

(18) Ischay, M. A.; Anzovino, M. E.; Du, J.; Yoon, T. P. *J. Am. Chem. Soc.* **2008**, *130*, 12886–12887.

(19) Tyson, E. L.; Ament, M. S.; Yoon, T. P. *J. Org. Chem.* **2013**, *78*, 2046–2050.

(20) Choi, W. J.; Choi, S.; Ohkubo, K.; Fukuzumi, S.; Cho, E. J.; You, Y. *Chem. Sci.* **2015**,

6, 1454–1464.

(21) Iqbal, N.; Choi, S.; Kim, E.; Cho, E. J. *J. Org. Chem.* **2012**, *77*, 11383–11387.

(22) Cismesia, M. A.; Yoon, T. P. *Chem. Sci.* **2015**, *6*, 5426–5434.

(23) Ismaili, H.; Pitre, S. P.; Scaiano, J. C. *Catal. Sci. Technol.* **2013**, *3*, 935–937.

(24) Pitre, S. P.; McTiernan, C. D.; Ismaili, H.; Scaiano, J. C. *J. Am. Chem. Soc.* **2013**, *135*, 13286–13289.

(25) Beatty, J. W.; Stephenson, C. R. J. *Acc. Chem. Res.* **2015**, *48*, 1474–1484.

(26) Yang, D. T.; Meng, Q. Y.; Zhong, J. J.; Xiang, M.; Liu, Q.; Wu, L. Z. *European J. Org. Chem.* **2013**, No. 33, 7528–7532.

(27) Wallentin, C. J.; Nguyen, J. D.; Finkbeiner, P.; Stephenson, C. R. J. *J. Am. Chem. Soc.* **2012**, *134*, 8875–8884.

(28) Hu, J.; Wang, J.; Nguyen, T. H.; Zheng, N. *Beilstein J. Org. Chem.* **2013**, *9*, 1977–2001.

(29) Yoon, U. C.; Mariano, P. S. *Acc. Chem. Res.* **1992**, *25*, 233–240.

(30) Lewis, F. D.; Ho, T. I.; Simpson, J. T. *J. Am. Chem. Soc.* **1982**, *104*, 1924–1929.

(31) Bergmark, W. R.; Whitten, D. G. *Mol. Cryst. Liq. Cryst.* **1991**, *194*, 239–245.

(32) Wightman, R. M.; Forry, S. P.; Maus, R.; Badocco, D.; Pastore, P. *J. Phys. Chem. B* **2004**, *108*, 19119–19125.

(33) Chow, Y. L.; Danen, W. C.; Nelsen, S. F.; Rosenblatt, D. H. *Chem. Rev.* **1978**, *78*, 243–274.

(34) Wayner, D. D. M.; McPhee, D. J.; Griller, D. *J. Am. Chem. Soc.* **1988**, *110*, 132–137.

(35) Ruiz Espelt, L.; McPherson, I. S.; Wiensch, E. M.; Yoon, T. P. *J. Am. Chem. Soc.* **2015**, *137*, 2452–2455.

(36) Miyake, Y.; Nakajima, K.; Nishibayashi, Y. *J. Am. Chem. Soc.* **2012**, *134*, 3338–3341.

(37) Zuo, Z.; Ahneman, D. T.; Chu, L.; Terrett, J. a.; Doyle, a. G.; MacMillan, D. W. C. *Science.* **2014**, *345*, 437–440.

(38) McNally, A.; Prier, C. K.; MacMillan, D. W. C. *Science.* **2011**, *334*, 1114–1117.

(39) Kohls, P.; Jadhav, D.; Pandey, G.; Reiser, O. *Org. Lett.* **2012**, *14*, 672–675.

(40) DeLaive, P. J.; DeLaive, P. J.; Lee, J. T.; Lee, J. T.; Abruna, H.; Abruna, H.; Sprintschnik, H. W.; Sprintschnik, H. W.; Meyer, T. J.; Meyer, T. J.; Whitten, D. G.; Whitten, D. G.; Wrighton, M.; Wrighton, M. *J. Am. Chem. Soc.* **1978**, *168*, 28–43.

(41) Monserrat, K.; Foreman, T. K.; Gratzel, M.; Whitten, D. G. *J. Am. Chem. Soc.* **1981**, *103*, 6667–6672.

(42) Maity, S.; Zheng, N. *Synlett* **2012**, *23*, 1851–1856.

(43) Condie, A. G.; González-Gómez, J. C.; Stephenson, C. R. J. *J. Am. Chem. Soc.* **2010**, *132*, 1464–1465.

(44) Freeman, D. B.; Furst, L.; Condie, A. G.; Stephenson, C. R. J. *Org. Lett.* **2012**, *14*, 94–97.

(45) Whitten, D. *Acc. Chem. Res.* **1980**, *286*, 83–90.

(46) Rueping, M.; Vila, C.; Koenigs, R. M.; Poscharny, K.; Fabry, D. C. *Chem. Commun. (Camb).* **2011**, *47*, 2360–2362.

(47) Cai, S.; Zhao, X.; Wang, X.; Liu, Q.; Li, Z.; Wang, D. Z. *Angew. Chemie - Int. Ed.* **2012**, *51*, 8050–8053.

(48) Lee, L. Y. . C.; Ci, X.; Giannotti, C.; Whitten*, D. G. *J. Am. Chem. Soc.* **1985**, *108*, 177–178.

(49) Yang, J.; Cauble, D. F.; Berro, A. J.; Bauld, N. L.; Krische, M. J. *J. Org. Chem.* **2004**, *69*, 7979–7984.

(50) Baik, T. G.; Luis, A. L.; Wang, L. C.; Krische, M. J. *J. Am. Chem. Soc.* **2001**, *123*, 6716–6717.

(51) Zimmerman, H.; Aasen, S. *J. Am. Chem. Soc.,* **1977***, 99,* 2342–2344.

(52) Hoffmann, N. *Chem. Rev.* **2008**, *108*, 1052–1103.

(53) Poplata, S.; Tröster, A.; Zou, Y.-Q.; Bach, T. *Chem. Rev.* **2016**, *Asap*.

(54) Loutfy, R. O.; Mayo, P. De. *Can. J. Chem.* **1974**, *52*, 3296–3296.

(55) Du, J.; Skubi, K. L.; Schultz, D. M.; Yoon, T. P. *Science* **2014**, *344*, 392–396.

(56) Oyama, M.; Goto, M.; Park, H. *Electrochem. Commun.* **2002**, *4*, 110–114.

(57) Rees, N. V.; Klymenko, O. V.; Compton, R. G.; Oyama, M. *J. Electroanal. Chem.* **2002**, *531*, 33–42.

(58) Bock, C. R.; Connor, J. A.; Gutierrez, A. R.; Meyer, T. J.; Whitten, D. G.; Sullivan, B. P.; Nagle, J. K. *J. Am. Chem. Soc.* **1979**, *101*, 4815–4824.

(59) Green, N. J. B.; Pimblott, S. M.; Tachiya, M. *J. Phys. Chem.* **1993**, *97*, 196–202.

(60) Lakowicz, J. R. *Principles of Fluorescence Spectroscopy*, 3rd ed.; 2006.

(61) Bock, C.; Meyer, T.; Whitten, D. *J. Am. Chem. Soc.* **1975**, *97*, 2909–2911.

(62) Gray, H. B.; Winkler, J. R. *Chem. Phys. Lett.* **2009**, *483*, 1–9.

(63) Khnayzer, R. S.; Thoi, V. S.; Nippe, M.; King, A.; Jurss, J. W.; El Roz, K. a.; Long, J. R.; Chang, C.; Castellano, F. N. *Energy Environ. Sci.* **2014**, *7*, 1477.

(64) Farnum, B. H.; Gardner, J. M.; Meyer, G. J. *Inorg. Chem.* **2010**, *49*, 10223–10225.

(65) Farnum, B. H.; Ward, W. M.; Meyer, G. J. *Inorg. Chem.* **2013**, *52*, 840–847.

(66) Stemp, E. D. A.; Arkin, M. R.; Barton, J. K. *J. Am. Chem. Soc.* **1997**, *119*, 2921–2925.

(67) Na, Y.; Pan, J.; Wang, M.; Sun, L. *Inorg. Chem.* **2007**, *46*, 3813–3815.

(68) Fukuzumi, S.; Kobayashi, T.; Suenobu, T. *Angew. Chemie - Int. Ed.* **2011**, *50*, 728–731.

(69) Brown, A. M.; McCusker, C. E.; McCusker, J. K. *Dalton Trans.* **2014**, *43*, 17635–17646.

(70) Barbante, G. J.; Kebede, N.; Hindson, C. M.; Doeven, E. H.; Zammit, E. M.; Hanson, G. R.; Hogan, C. F.; Francis, P. S. *Chemistry* **2014**, *20*, 14026–14031.

(71) Desimone, R. E.; Drago, R. S. **1969**, *3442*, 2343–2352.

(72) Biner, M.; Buergi, H. B.; Ludi, a.; Roehr, C. *J. Am. Chem. Soc.* **1992**, *114*, 5197–5203.

(73) Ghosh, P. K.; Brunschwig, B. S.; Chou, M.; Creutz, C.; Sutin, N. *J. Am. Chem. Soc.* **1984**, *106*, 4772–4783.

(74) Yin, Q.; Tan, J. M.; Besson, C.; Geletii, Y. V; Musaev, D. G.; Kuznetsov, A. E.; Luo, Z.; Hardcastle, K. I.; Hill, C. L. *Science.* **2010**, *328*, 342–345.

(75) Lv, H.; Song, J.; Geletii, Y. V.; Vickers, J. W.; Sumliner, J. M.; Musaev, D. G.; Kögerler, P.; Zhuk, P. F.; Bacsa, J.; Zhu, G.; Hill, C. L. *J. Am. Chem. Soc.* **2014**, *136*, 9268–9271.

(76) Yin, Q.; Tan, J. M.; Besson, C.; Geletii, Y. V.; Musaev, D. G.; Kuznetsov, a. E.; Luo, Z.; Hardcastle, K. I.; Hill, C. L. *Science.* **2010**, *328*, 342–345.

(77) Xu, X.; Shreder, K.; Iverson, B. L.; Bard, A. J. *J. Am. Chem. Soc.* **1996**, *118*, 3656–3660.

(78) Goez, M.; von Ramin-Marro, D.; Othman Musa, M. H.; Schiewek, M. *J. Phys. Chem. A* **2004**, *108*, 1090–1100.

(79) Kanoufi, F.; Zu, Y.; Bard, a. J. *J. Phys. Chem. B.* **2001**, *105*, 210–216.

APPENDIX

Control Experiments

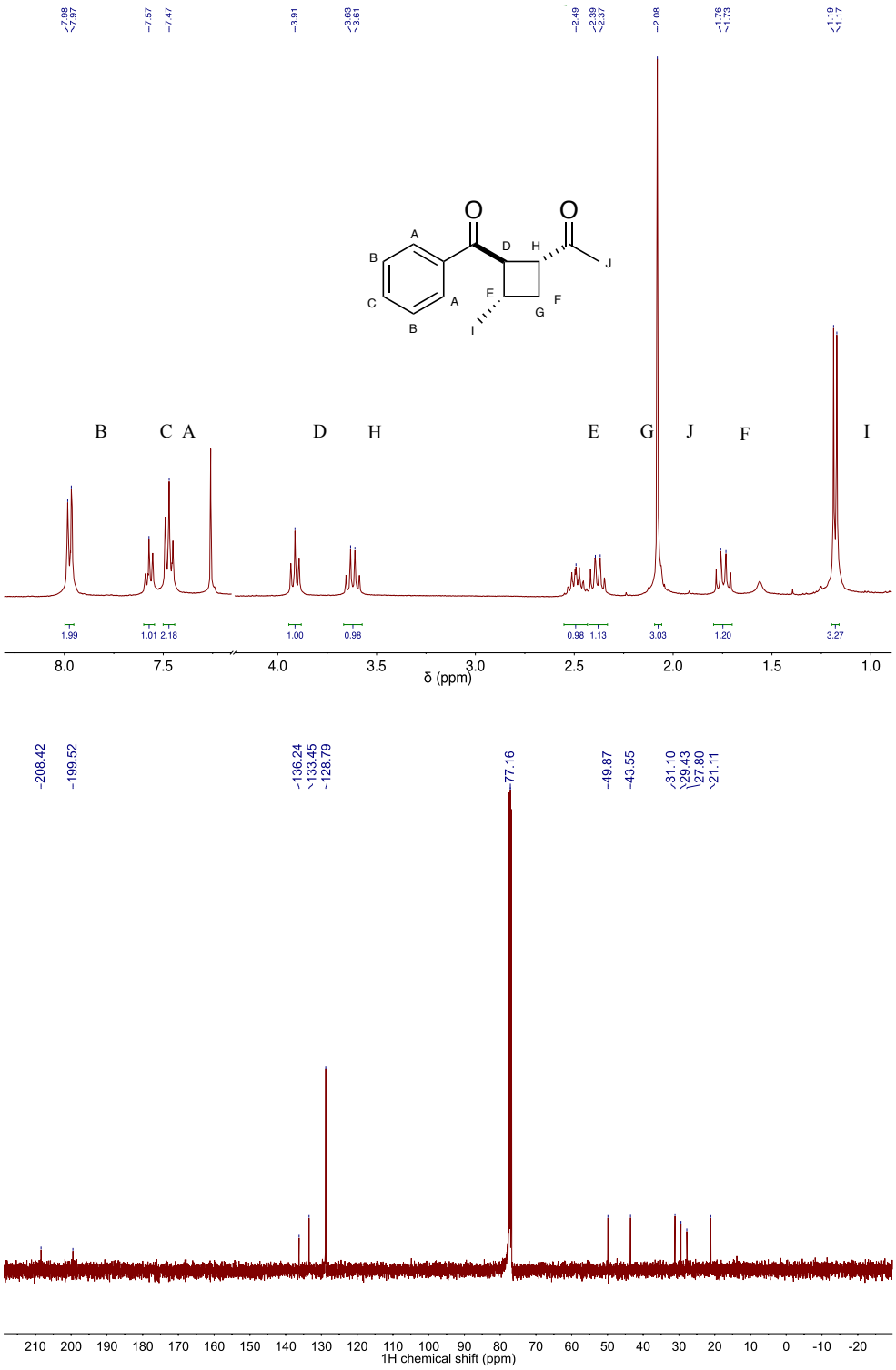

Figure S1. ^{1}H NMR ($CDCl_3$, 400 MHz, top) and ^{13}C NMR ($CDCl_3$, 100 MHz, bottom) spectra of trans-cyclobutane (**3**).

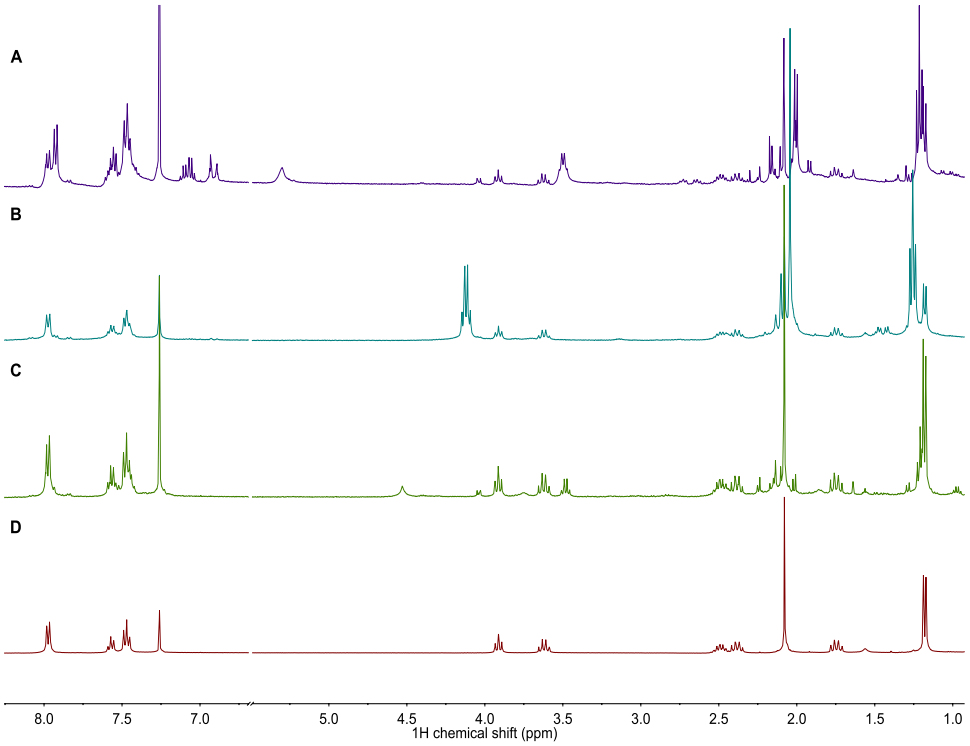

Figure S2. ^{1}H NMR ($CDCl_3$, 400 MHz) spectra of reaction crude: a) $[Ru(bpy)_3]^{2+}$ with TEA; b) *fac*-$Ir(ppy)_3$ with DIPEA; c) $[Ru(bpy)_3]^{2+}$ with DIPEA; d) **3.**

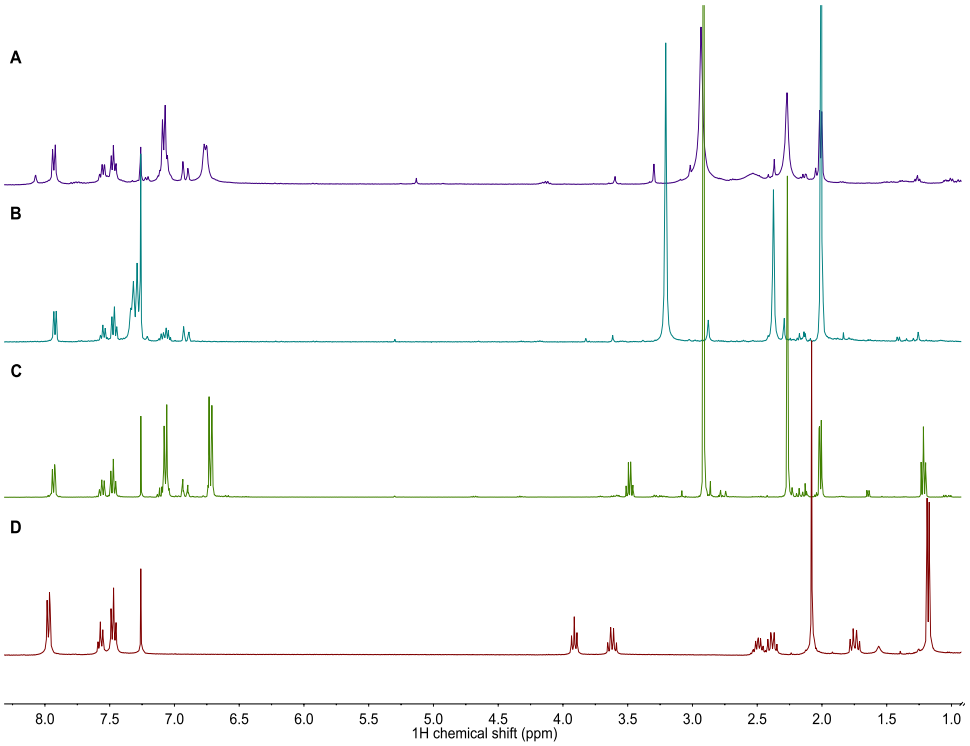

Figure S3. ^{1}H NMR ($CDCl_3$, 400 MHz) spectra a) $[Cu(dsbp)_2]^{+}$ with DMT; b) *fac*-$Ir(ppy)_3$; c) $[Ru(bpy)_3]^{2+}$ with DMT; d) **3.**

Stern-Volmer data

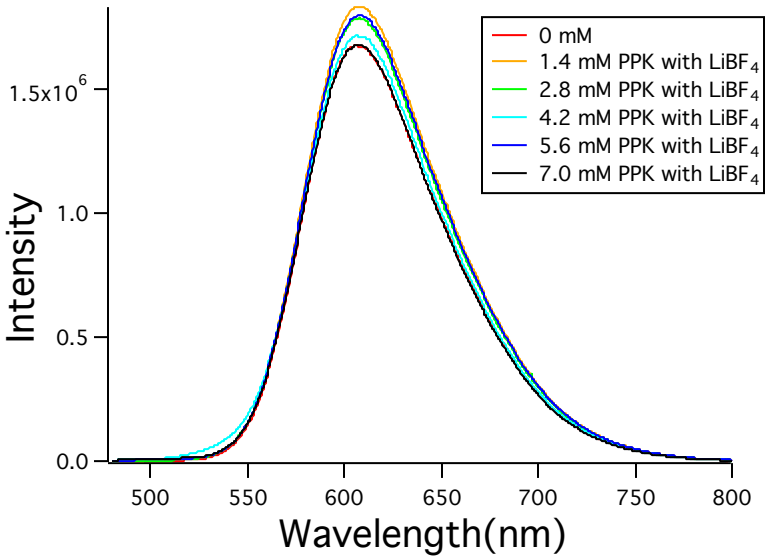

Figure S4. Luminescence quenching of 0.01 mM $[Ru(bpy)_3]^{2+}$ by **1**[a]

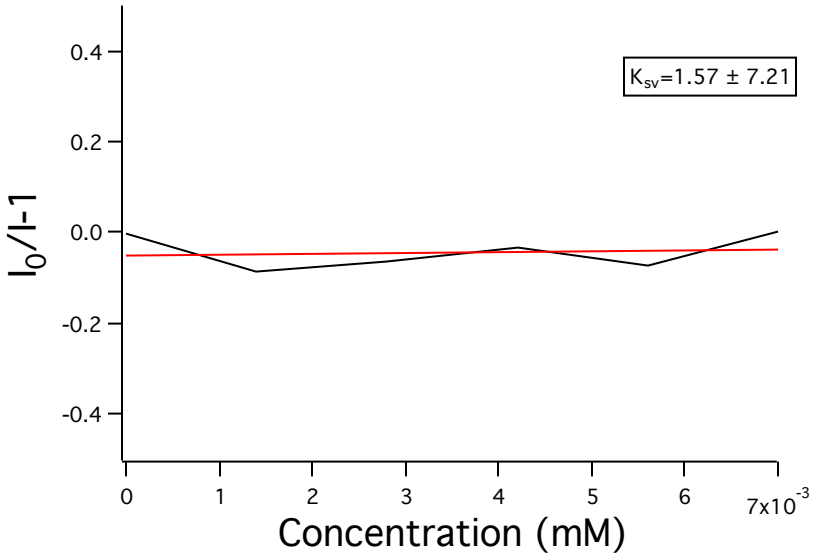

Figure S5. Stern-Volmer Plot between 0.01 mM $[Ru(bpy)_3]^{2+}$ by **1**[a]

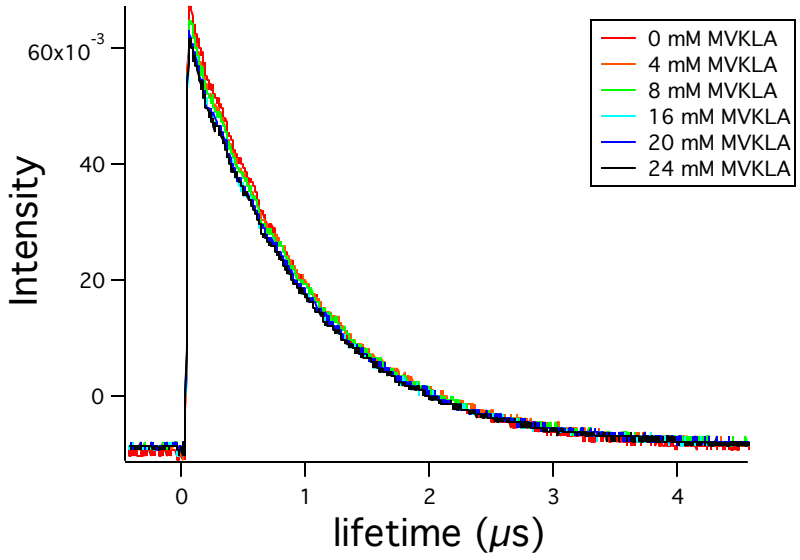

Figure S6. Lifetime quenching of 0.01 mM $[Ru(bpy)_3]^{2+}$ by **2**[a] and its Stern-Volmer plot

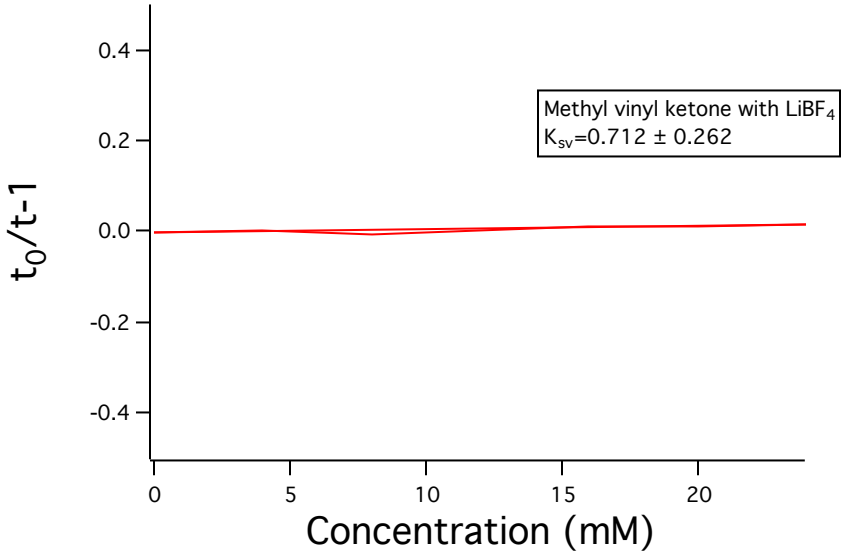

Figure S7. Stern-Volmer Plot between 0.01 mM $[Ru(bpy)_3]^{2+}$ by **2**[a]

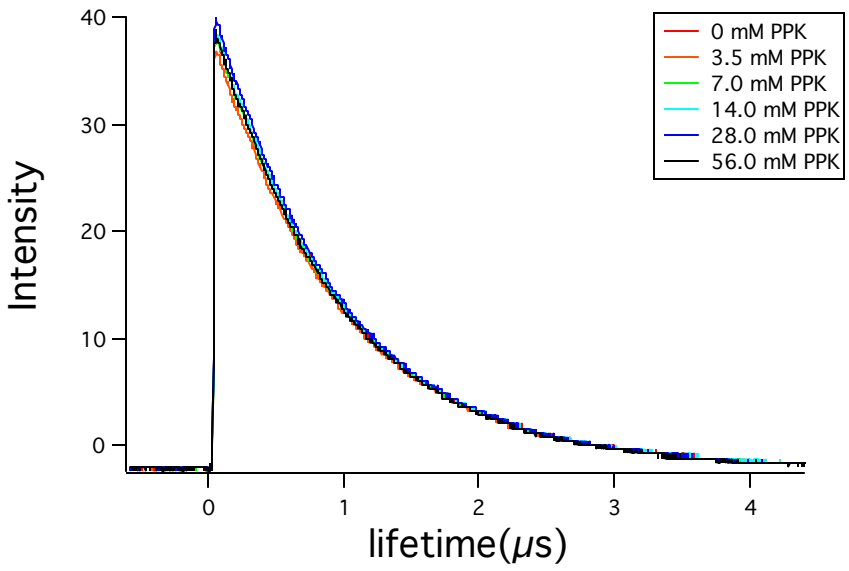

Figure S8. Lifetime quenching of 0.01 mM $[Ru(bpy)_3]^{2+}$ by **1**

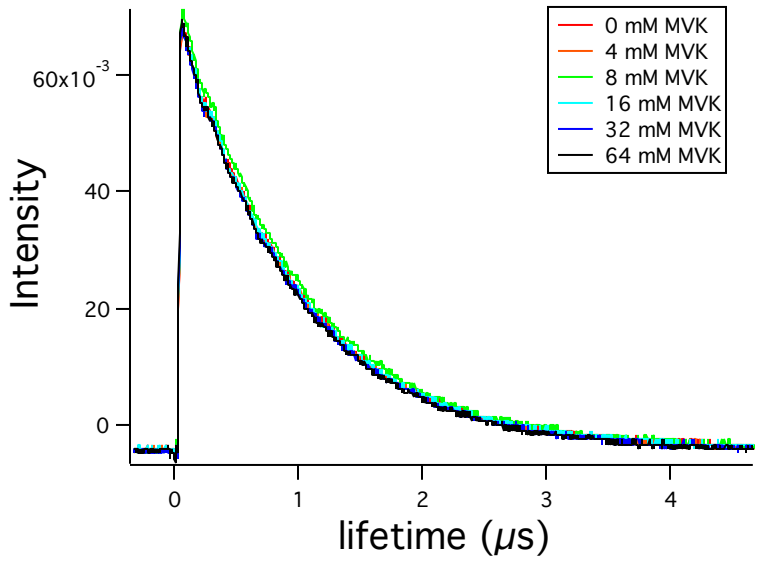

Figure S9. Lifetime quenching of 0.01 mM $[Ru(bpy)_3]^{2+}$ by **2**

Electrochemistry

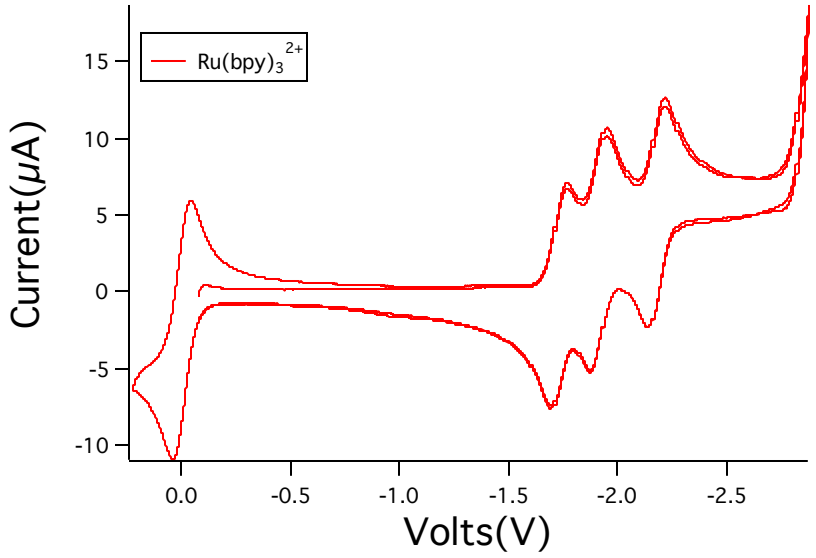

Figure S10. Cyclic voltammogram of $Ru(bpy)_3^{2+}$ in 0.1M $TBABF_4$ in DMF. $Fc^{+/0}$ was used as internal reference

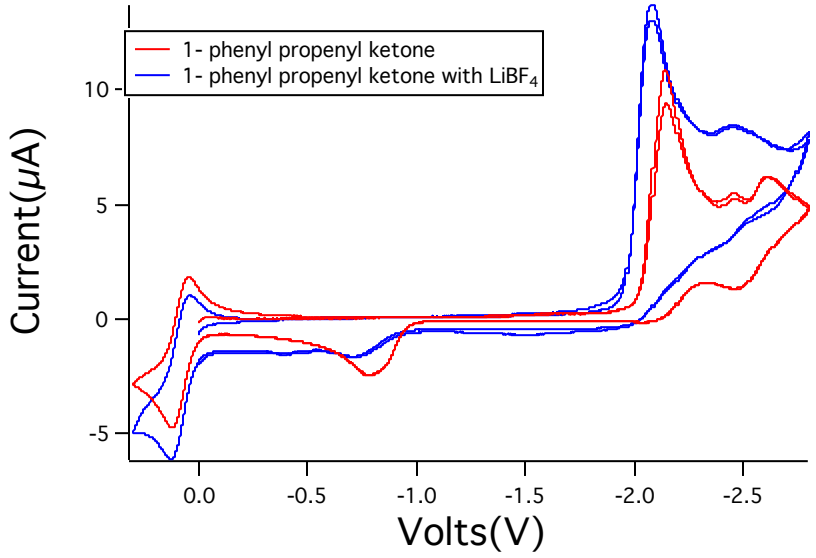

Figure S11. Cyclic voltammogram of phenyl 1-propenyl ketone (**1**), and phenyl 1-propenyl ketone with $LiBF_4$ (**1**[a]) in 0.1M $TBABF_4$ in DMF. $Fc^{+/0}$ was used as internal reference

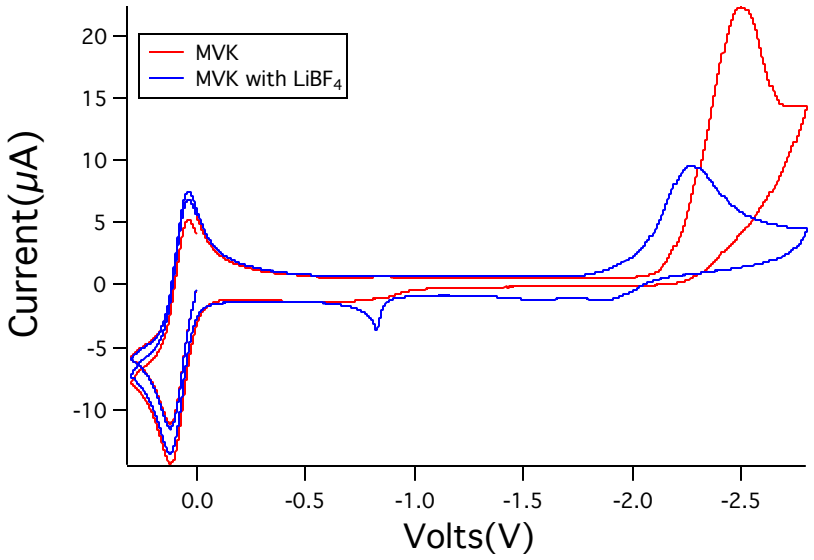

Figure S12. Cyclic voltammogram of methyl vinyl ketone with $LiBF_4$ (**2**[a]) in 0.1M $TBABF_4$ in DMF. $Fc^{+/0}$ was used as internal reference